Chemistry and Physics of Lipids 157 (2009) 61–77

Contents lists available at ScienceDirect

Chemistry and Physics of Lipids

journal homepage: www.elsevier.com/locate/chemphyslip

Review

Membrane lipid domains and rafts: current applications of fluorescence lifetime spectroscopy and imaging

Rodrigo F.M. de Almeida[a,*], Luís M.S. Loura[b,c], Manuel Prieto[d]

[a] Centro de Química e Bioquímica, Faculdade de Ciências da Universidade de Lisboa, R. Ernesto de Vasconcelos, 1749-016 Lisboa, Portugal
[b] Faculdade de Farmácia, Universidade de Coimbra, Rua do Norte, 3000-295 Coimbra, Portugal
[c] Centro de Química de Évora, Rua Romão Ramalho, 59, 7000-671 Évora, Portugal
[d] Centro de Química-Física Molecular and Institute of Nanosciences and Nanotechnologies, Complexo I, Instituto Superior Técnico, Av. Rovisco Pais, 1049-001 Lisboa, Portugal

ARTICLE INFO

Article history:
Received 2 June 2008
Accepted 24 July 2008
Available online 3 August 2008

Keywords:
FLIM
FRET
Fluorescence microscopy
Protein–membrane interactions
Sphingomyelin–cholesterol domains
Ceramide

ABSTRACT

Membrane microdomains and their involvement in cellular processes are part of the current paradigm of biomembranes. However, a better characterization of domains, namely lipid rafts, is needed. In this review, it is shown how the use of time-resolved fluorescence, with the adequate parameters and probes, helps elucidating the type, number, fraction, composition and size of lipid phases and domains in multicomponent model systems. The determination of phase diagrams for lipid mixtures containing sphingolipids and/or cholesterol is exemplified. The use of fluorescence quenching and Förster resonance energy transfer (FRET) are also illustrated. Strategies for studying protein-induced domains are presented. The advantages of using single point microscopic decays and fluorescence lifetime imaging microscopy (FLIM) in systems with three-phase coexistence are explained. Finally, the introduction of FLIM allows studies in live cell membranes, and the nature of the microdomains observed is readily elucidated due to the information retrieved from fluorescence lifetimes.

Contents

1. Introduction

The study of lipid–lipid interactions in general, and the formation and properties of lipid domains in particular, from the nano to the microscale, are by now an established field in Membrane Biophysics and Biochemistry (e.g. Edidin, 2003; Mukherjee and Maxfield, 2004; Kusumi et al., 2005; Anderson and Jacobson, 2002). The suggestion of lipid segregation as one of the basic mechanisms of cellular lipid and protein trafficking and sorting goes back to the 1980s (Simons and Van Meer, 1988) and early 90s (Bretscher and Munro, 1993). The most actively studied type of lipid domains is known as lipid rafts,

* Corresponding author. Tel.: +351 21 7500865.
E-mail address: rodrigo.almeida@fc.ul.pt (R.F.M. de Almeida).

0009-3084/$ – see front matter © 2008 Elsevier Ireland Ltd. All rights reserved.
doi:10.1016/j.chemphyslip.2008.07.011

which are thought to consist of sphingolipid–cholesterol (Chol)-enriched and (unsaturated) phosphatidylcholine (PC)-depleted domains. In general it is considered, in the context of this review, lipid domains as lateral membrane heterogeneity generated on the basis of differential lipid–lipid and specific lipid–protein interactions. The role of lipid transversal asymmetry and the general roles of proteins have been reviewed elsewhere (Devaux and Morris, 2004; Pérez-Gil et al., 2006; Epand, 2006).

Rafts in a rest state in cell membranes seem to be in general <100 nm (e.g. Varma and Mayor, 1998; Prior et al., 2003; Nicolau et al., 2006; Sengupta et al., 2007). However, the recent studies in model systems with more impact have been the direct microscopic observation of micrometer-scale liquid/liquid immiscibility (e.g. Dietrich et al., 2001). Certainly this is related to the fact that many studies in cells are performed with fluorescence microscopy, and the observation of giant vesicles allows using approaches frequently employed in Cell Biology. Not uncommonly, though, the results from experiments with these techniques do not show any domains for compositions for which spectroscopic ensemble techniques preview phase separation (e.g. binary systems PC/Chol; Dietrich et al., 2001; Veatch and Keller, 2003). This and other complexities led to the development of more sophisticated approaches, where the combination of spectroscopic data with imaging of the lipid bilayer became essential, e.g. the use of laurdan spectral shifts (Bagatolli and Gratton, 2000; Dietrich et al., 2001), of fluorescence correlation spectroscopy (FCS) (Kahya and Schwille, 2006; Ruan et al., 2004), or of NMR (Veatch et al., 2007).

Fluorescence spectroscopy has been used to address all these subjects for a long time, due to its intrinsic sensitivity, which is a major advantage in biological systems (e.g. Prenner et al., 1993, 2000), and also because the time-scale of fluorescence emission together with the time-resolution of detection allow obtaining dynamical information (e.g. Sharma et al., 1997). Several types of parameters can be used, such as fluorescence lifetimes, anisotropy decays (Ravichandra and Joshi, 1999) and time-resolved emission spectra (e.g. Parasassi et al., 1993). Since they depend on different characteristics of the probe environment, like polarity or microviscosity, they can report the appearance of new phases which otherwise would not be detected. By combining these parameters with the direct observation of heterogeneities through imaging techniques, fluorescence methods with time-resolution are one of the potentially most useful tools to study lipid domains and rafts. It should also be stressed that time-resolved techniques have the advantage of not evaluating the total intensity, so they are much less biased by the known problems associated to steady-state data such as light scattering, or error in probe concentration. However, this combination has not been widely used thus far. One of the reasons is that in order to safely conclude from the time-resolved fluorescence properties of the probes in complex systems, it is previously mandatory to know in detail the photophysical properties of the probe(s) in membrane model systems with different number of components and compositions, mimicking the several types of lipid phases and domains that can be present in the cell membranes.

This chapter will focus on the information that can be drawn directly from examination of fluorescence lifetimes, and the parameters calculated from them (Förster resonance energy transfer (FRET) efficiency, dynamic quenching and partition coefficients), and their combination with imaging (fluorescence lifetime imaging microscopy (FLIM)). Examples of applications will range from two-component model systems to studies in live cells.

2. Lipid–lipid and lipid–protein interactions studied by time-resolved fluorescence: techniques and methods

2.1. Introducing time-resolved fluorescence

Here, brief comments mainly of practical nature are drawn, and for a more complete discussion of fluorescence spectroscopy, the reader is referred to two comprehensive textbooks (Valeur, 2001; Lakowicz, 2006).

In steady-state fluorescence spectroscopy, as carried out in a spectrofluorimeter, continuous illumination is provided by the light source (often a Xe arc lamp). Hence, the concentration of molecules in the electronic excited state (and therefore the emission intensity) is proportional to the intensity of absorbed excitation light. By varying the excitation or emission wavelengths, it is easy to measure fluorescence spectra. On the other hand, in time-resolved fluorescence spectroscopy, the fluorescence decay curve of a fluorophore in a sample is measured. The relationship between the steady-state fluorescence intensity I of a given fluorophore and its decay law $i(t)$ (which is obtained from a time-resolved experiment) is rather simple, as the former is the integration over time of the latter:

$$I = \int_0^\infty i(t)\,\mathrm{d}t \tag{1}$$

This means that I represents an intensity value averaged over all fluorophores of the sample and all times, whereas the decay law is a function of time, only averaged over fluorophores. It follows that a single steady-state intensity value is probably determined by several decay law parameters, which cannot be extracted from it. In fact, it is not rare that, for a given situation, the decay law model allows distinct sets of parameters leading to identical steady-state intensity values. On the other hand, the experimental decay is typically composed of ~1000 data points, and fitting a model decay law to the experimental histogram provides the parameters of interest in a unique and statistically meaningful manner. Finally, steady-state but not time-resolved measurements are subject to inner-filter artifacts which, when present, must be corrected (Coutinho and Prieto, 1993).

Time-resolved experiments are often performed through direct measurements in the time domain, in which a short pulse of light excites the sample, and the subsequent fluorescence emission is recorded as a function of time. This is generally achieved using time-correlated single photon counting (TCSPC), which uses electronics to detect single-photon events at a detector. By repeating many start-stop signals, a histogram of single-photon counts in discrete time channels is obtained (O'Connor and Phillips, 1984). Alternatively, the frequency-response of the emission to intensity-modulated excitation can be used to obtain the time-dependent decay in frequency domain time-resolved fluorescence spectroscopy. Below we will focus briefly on experimental details regarding the time-domain variant.

The technique of TCSPC consists in exciting the sample and detecting the arrival time of the first emitted photon. Therefore, this technique is also called single photon timing (SPT). Since the detection rate is very low, i.e. one photon is detected for ~100 excitation pulses in order to avoid biasing to shorter times, the experiment must be repeated many times, so high repetition sources are needed.

During recent times, time-domain instrumentation has become more accessible, and it is possible to have high quality, user-friendly systems, without using expensive equipment. The state-of-the-art instrumentation uses high repetition rate mode-locked picosecond or femtosecond lasers as excitation sources, and detection is carried out by high-speed photomultipliers, the microchannel plates

(MCPs). For less demanding studies the former can be successfully replaced by the less expensive pulsed-laser diodes (LDs) or light-emitting diodes (LEDs). At the same time, fast standard photomultipliers can be used. Dye lasers pumped by argon-ion lasers were invaluable in TCSPC, and they are still widely used, essentially for exciting fluorophores that absorb the frequency-doubled output of the dye emission. They have also intrinsically narrow pulse profiles (~5 ps) and can be tuned in wavelength, although they are complex to operate. At present these lasers are being replaced by solid-state lasers (e.g. Ti–sapphire, which must be pumped by a primary laser of solid-state diode lasers), which are more friendly to operate and have shorter time-pulse (~100 fs) and high power which allows multi-photon excitation. For this reason they became popular in microscopy for FLIM studies, where localized excitation at a focal point is an advantage. However, it should be stressed that for UV excitation in the spectral region of tryptophan (Trp) absorption the doubled frequency dye laser is still the best source.

Recent progress in LDs and LEDs allow time-domain studies at a very reasonable budget as described above. In addition, they are very easy to operate, maintenance-free and the pulse width of a LD (~50 ps) is excellent for the decay of most probes in biophysics. LEDs are even less expensive, and although they do not have a tunable region for excitation, and the pulse width is one order of magnitude larger, they allow reasonably quick data acquisition. At present these sources are available in a whole collection of wavelengths, including the UV, allowing, e.g. studies with Trp.

2.2. How to deal with the complex fluorescence of membrane probes

In a microheterogeneous medium the decay of a fluorophore is usually not described by a single exponential function (complex decay kinetics) (e.g. Visser et al., 1988). This can be a result of the intrinsic photophysics, but even the emission of a fluorophore which in homogeneous medium presents a single-exponential decay, usually becomes complex when incorporated in a membrane. This happens because of the contribution of several sub-populations, since in the case of a fluorophore adsorbed at the membrane–water interface, different micro-environments varying in polarity and viscosity exist, and in addition solvent relaxation within each of the populations can add further complexity. This heterogeneity can be described by a distribution of lifetimes, either Gaussian or obtained from non a priori methods such as Maximum Entropy. The broadness of the distribution gives some insight on the degree of heterogeneity.

In sum, the usual situation is that any probe, even when in interaction with vesicles where there is a single phase present, has a complex decay with several components. In case that there is phase co-existence (e.g. the probe is partitioned between two phases, either gel/fluid or liquid ordered (l_o)/liquid disordered (l_d)) there is an added complexity, and in general the lifetime components can not be attributed to the phases, although some exceptions will be shown later (in these cases, a very careful and detailed data analysis is required).

When the fluorescent probe is participating as a donor in a FRET interaction (see next section), specific non-exponential decay laws apply (Loura et al., 2001a), since in membranes in general donor and acceptor molecules are distributed in the membrane and the distance between all possible donor and acceptor molecules can take many different values. Furthermore, the acceptor probes can have random or non-random distributions in the membrane. However, even in this situation a sum of exponentials is very effective in describing the decay kinetics and their number is only determined by the satisfaction of the usual statistical criteria (low chi-square, random distribution of residuals and their auto-correlation). No physical meaning is attributed to the different components, and this discrete approach allows complex FRET kinetics to be used, assuming that transfer operates from different states with distinct lifetimes.

Sometimes, due to the obscure physical meaning of each exponential used in the fit to the experimental decay curve, it is useful to describe the fluorescence kinetics through a parameter named mean or average lifetime, given by

$$< \tau >= \frac{\left(\sum_i \alpha_i \tau_i^2\right)}{\left(\sum_i \alpha_i \tau_i\right)} \tag{2}$$

for a decay described by a sum of exponentials, where α_i is the normalized pre-exponential and τ_i the lifetime of the decay component i. This parameter, for some probes, is very sensitive to lipid phase transitions, but should not be used in all cases where the interaction under study is dependent on the quantum yield, such as will be shown in the next section, namely regarding the determination of partition coefficients. In these cases the so-called lifetime weighted quantum yield (Lakowicz, 2006), also designated by amplitude averaged lifetime defined as

$$\bar{\tau} = \sum_i \alpha_i \tau_i \tag{3}$$

is the relevant one.

2.3. Information contained in fluorescence lifetimes: dynamic quenching and FRET efficiency; probe preference for lipid domains

When the phase diagram for a lipid system is known, including the tie-lines (i.e., a line connecting the compositions of two phases which are in equilibrium over all that line) that contain the lipid mixtures of concern, quantitative characterization of the lipid domains can be made. The tie-lines are horizontal in a binary system (T or pressure/composition phase diagram), but in case of a ternary system, in the phase diagram, the so-called Gibbs triangle, the tie-lines are no longer horizontal, and thus they must be obtained experimentally, which can be a very complex and time-consuming task. The lever rule is valid in both cases and the amount and composition of each phase can be computed. From the restrictions imposed by thermodynamics and the minimization of the deviation between fluorescence parameters that are calculated from the phase diagram and the experimentally determined ones, the tie-lines in ternary systems can be determined with very small uncertainty, as is the case of the phase diagram shown in Fig. 1 (Castro et al., 2007). The advantage of carrying out the study along a tie-line is that the composition of each coexisting phase is invariant.

To quantify the preference of a molecule (a fluorescent probe, a protein, etc.) for different lipid phases, the probe partition coefficient, K_p, has to be obtained. The partition coefficient of a probe between phase 2 and phase 1 is defined as

$$K_p = \frac{n_2/X_2}{n_1/X_1} \tag{4}$$

where n_1 and n_2 are the number of mole of probe in phase 1 and 2, respectively, and X_i the mole fraction of phase i. A preference for phase 2 corresponds to $K_p > 1$, for phase 1 to $K_p < 1$, and if $K_p \sim 1$ there is no marked preference of the probe between any phase.

Phases 1 and 2 are any two co-existing lipid phases, usually gel and fluid or l_o and l_d, and K_p is meaningful only when a tie-line is considered. Fluorescence lifetime data can be used to quantitatively

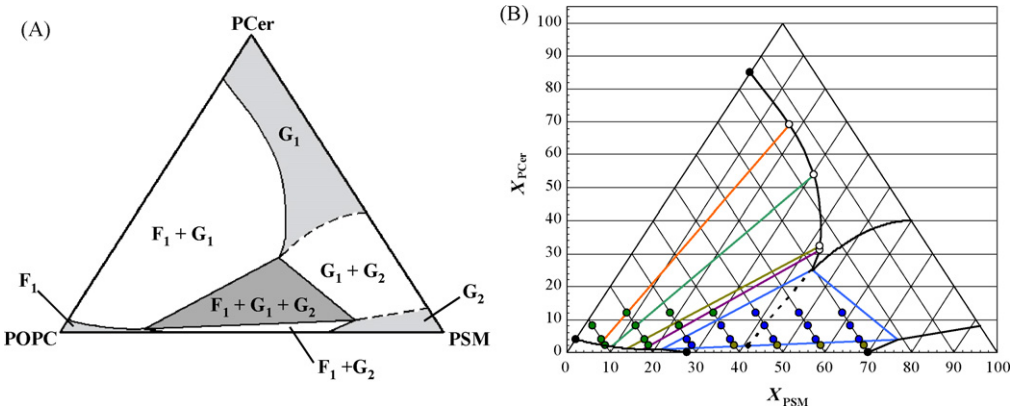

Fig. 1. PSM/POPC/PCer ternary phase diagram at 24 °C. (A) Identification of the regions of the phase diagram. The abbreviations correspond to: F1, POPC-rich fluid phase; G1, PCer-rich gel, and G2, PSM-rich gel phase. The colours correspond to the number of phases present in each region: light gray, one phase; white, two phases; dark gray, three phases. (B) Scaled POPC/PSM/PCer phase diagram. The black lines represent the phase boundaries between one-phase and two-phase regions. Each side of the tie-triangle (blue) is a phase boundary that separates a two-phase region from a three-phase region. The remaining coloured lines are experimental tie-lines for the F1 + G1 region. The open and closed circles over the black curved lines are the edges of the tie-lines. The direction and length of these tie-lines were obtained from the fraction of each phase calculated from *t*-PnA lifetime and the lever rule. The black points on the left and bottom sides of the diagram are experimental points taken from the POPC/PCer (Silva et al., 2006a,b) and the POPC/PSM (de Almeida et al., 2003) phase diagrams, respectively. The lipid mixtures studied are the coloured points. In each of them, phase coexistence was experimentally verified and quantified: dark green – POPC-rich fluid and PCer-rich gel phases; light green – PCer-rich gel and PSM-rich gel phases; blue – the three phases. Adapted from Castro et al., 2007.

determine partition coefficients. The relevant expression when no significant spectral shifts occur is:

$$\bar{\tau} = \frac{(\bar{\tau}_1 K_p X_1 + \bar{\tau}_2 X_2)}{(K_p X_1 + X_2)} \quad (5)$$

where $\bar{\tau}_i$ is the lifetime-weighted quantum yield of the probe in phase *i*. From a non-linear fit of Eq. (5) to $\bar{\tau}$ versus X_2 data, K_p is readily obtained. Examples are given in Fig. 2.

In some cases, the variation of the average fluorescence lifetime is much more pronounced than that of the lifetime-weighted quantum yield. In this case estimating K_p from the former parameter yields a more reliable value than from the latter. The equation to use is now,

$$< \tau >= \frac{< \tau >_1 K_p X_1 + \bar{\tau}_2/\bar{\tau}_1 < \tau >_2 X_2}{K_p X_1 + \bar{\tau}_2/\bar{\tau}_1 X_2} \quad (6)$$

Table 1 shows K_p values for different probes and lipid systems obtained from lifetime variation, using either Eq. (5) or Eq. (6). For alternative methods that allow obtaining relative partition constants between series of fluorophores see (Silvius, 2005).

FRET is a dipolar interaction between two molecules, in which excitation energy is transferred (non-radiatively) from one molecule (the donor) to another (the acceptor), with a distance-dependent rate constant, and its efficiency, *E*, can be easily determined from lifetime data:

$$E == 1 - \frac{\bar{\tau}_{DA}}{\bar{\tau}_D} \quad (7)$$

where $\bar{\tau}_D$ and $\bar{\tau}_{DA}$ are the lifetime-weighted quantum yield of the donor in the absence and presence of acceptor, respectively.

From the independent knowledge of the probes' (donor and acceptor) partition coefficients, equations can be used which enable the estimation of the domain sizes. This is a fundamental question, because membrane lipid domains are at the verge of detection by different techniques and this has to be taken into account when interpreting biophysical data (Filippov et al., 2007). The mathematics for FRET in membrane model systems and their application to the study of lipid heterogeneity were reviewed in greater detail elsewhere (Loura et al., 2001a; Towles et al., 2007; Buboltz, 2007). Briefly, when the domains are very large regarding the Förster radius, R_0, the so-called infinite phase separation limit (Fig. 3C), a minimum of FRET efficiency is attained for a FRET pair with donor and acceptor preferring different phases. On the other hand, if the domains are very small (Fig. 3A), no decrease in efficiency is observed, i.e. a close to random probe distribution happens (as if only one phase were present).

In between the two limits described above, we have the biologically relevant situation of domains in the tenths of nanometer size (Fig. 3B). In this situation, donors in one phase, in addition to transfer to acceptors in the same phase, can also interact with acceptors

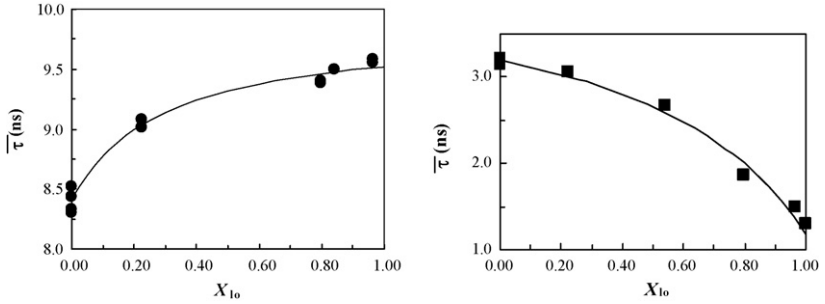

Fig. 2. Variation of lifetime weighted quantum yield of: (A) NBD-DPPE and (B) Rhodamine-DOPE in PSM/POPC/Chol large unilamellar vesicles, as a function of lo phase mole fraction, along the tie-line that contains the lipid mixture 1:1:1 (mol:mol:mol) at 23 °C (see Fig. 5B). The lines are the fitting curves of Eq. (5) with l_o/l_d partition coefficient $K_p = 4.3 \pm 1.2$ (NBD-DPPE) and $K_p = 0.37 \pm 0.06$ (Rhodamine-DOPE). Adapted from de Almeida et al. (2005).

Table 1
Partition coefficients of membrane probes in different lipid mixtures and phase coexistence situations, determined from the variation of the fluorescence lifetime of the probe (Eqs. (5) and (6)) at room temperature (22–24 °C), unless otherwise indicated. The fluorescence lifetime of the probes in each of the coexisting phases (1 and 2), i.e. on the tie-line extremes, are also given

Probe	Lipid mixture	Phases 1/2	K_p 1/2	τ_1(ns)[a]	τ_2 (ns)[a]	References
t-	DSPC/DLPC	Gel/fluid	4.8 ± 0.5	56.4	4.7	de Almeida et al. (2002)
PnA	PCer/POPC	Gel/fluid	4.5 ± 0.6	*37*	*5*	Silva et al. (2006b)
	POPC/Chol	l_o/l_d	0.8 ± 0.2	*12*	*5*	Mateo et al. (1995), de Almeida et al. (2004)
	POPC/PSM/Chol[b]	l_o/l_d	0.88 ± 0.05	*17*	*6*	Silva et al. (2007)
	PSM/POPC	Gel/fluid	1.9 ± 0.1	*32*	*12*	Castro et al. (2007)
	PCer/PSM	Gel/gel[c]	2.4	*37*	*32*	Castro et al. (2007)
NBD-DPPE[d]	POPC/PSM/Chol[a]	l_o/l_d	4.1 ± 0.9	8.4	9.5	de Almeida et al. (2005); Silva et al. (2007)
NBD-DOPE[d]	POPC/PSM/chol[a]	l_o/l_d	1.20 ± 0.06	6.3	5.5	Silva et al. (2007)
	PCer/POPC	Gel/fluid	~0[e]	n. a.	5	Silva et al. (2006b)
1-C_{16}-2-NBD-C_{12}-PC[d]	DPPS/DPPC at 45 °C	Gel/fluid	0.31 ± 0.06	3.28	4.42	Loura et al. (2006)
Rhod-	DPPC/DOPC	Gel/fluid	0.17 ± 0.07[f]	2.6	2.6	de Almeida et al. (2007)
DOPE[d]	DPPC/Chol	Gel/lo	0.5 ± 0.1	2.6	1.9	de Almeida et al. (2007)
	POPC/PSM/chol[a]	l_o/l_d	0.34 ± 0.07	3.1	1.4	de Almeida et al. (2005, 2007)
Rhod-DMPE[d]	DMPC/Chol (30 °C)	l_o/l_d	0.30	2.7	1.5	Loura et al. (2001c)
DPH	PCer/POPC	Gel/fluid	~0[e]	n. a.	*5*	Silva et al. (2006b)
$DiIC_{12}$	DSPC/DLPC	Gel/fluid	0.5	1.06	0.74	Loura et al. (2000)
$DiIC_{18}$	DSPC/DLPC	Gel/fluid	5.2	1.40	0.74	Loura et al. (2000)

[a] Lifetime-weighted quantum yields are in normal letter; average fluorescence lifetimes are italicized.
[b] For the tie-line that contains the 1:1:1 mol ratio mixture.
[c] Because the variation of fluorescence lifetime between these two lipid-phases is very small, the K_p was calculated indirectly from the ratio of the K_p in the PCer/POPC and PSM/POPC systems.
[d] For these probes, the fluorescence lifetime may change significantly with the probe:lipid ratio due to a dynamic self-quenching process. This dependence will also be influenced by the lateral diffusion coefficient and the molecular area of the lipids.
[e] The photophysical parameters of these probes remain almost unchanged with PCer mole fraction indicating that their partition into the PCer-rich gel phase is very low.
[f] Because the fluorescence lifetime of the probe is the same in both lipid phases at low probe:lipid ratio, this K_p value was calculated as the product of the K_p values given in the two following lines.

located in the other one. In this case, the experimental efficiency is higher as compared to the situation of "infinite phase separation", but lower than in a single homogeneous phase where a random distribution of probes can be anticipated. It will be shown later in this chapter how this method allowed establishing the lipid rafts size variation with membrane composition.

Together with FRET, quenching is the most common methodology in the area of biological applications of fluorescence. In case that fluorescence quenching is a dynamic process, i.e. diffusion dependent, in biological systems, specifically both fluorophore and quencher diffusing in a membrane, "transient effects" due to diffusion can not be studied in detail due to the following: (i) diffusion is no longer isotropic, and at least two different components, parallel and perpendicular to the membrane plane, should be taken into account, which leads in general to a formalism of no practical use, (ii) the decay of most samples, even in the absence of quencher, is intrinsically complex (see previous section).

Thus, the Stern–Volmer equation is in most situations the starting point, and from time-resolved data a linear relationship (Eq. (8)) should be obtained,

$$\frac{\bar{\tau}_0}{\bar{\tau}} = 1 + k_q < \tau >_0 [Q] \tag{8}$$

where τ_0 and τ are the fluorescence lifetimes in the absence and presence of the quencher, k_q is the bimolecular collisional rate constant, and [Q] is the effective quencher concentration in the membrane. This rate constant can be used to obtain the diffusion coefficient D (see the approximation of Umberger and Lamer, 1945).

To deal with the complex intrinsic decay of most fluorophores, generally the quenching of each component cannot be detailed, and the use of mean or average lifetimes, which is not uncommon to find described in a wrong way in the literature, is the usual approach. In the above Eq. (8), the lifetime-weighted quantum yields (see Eq. (3)) should be used on the left-hand side of the equation, while the mean lifetime should be used on the right-hand side. This last one in fact describes the mean time that the molecule spends in the excited state, so is the relevant one to consider in diffusional processes. It can be even more refined such as described by Sillen and

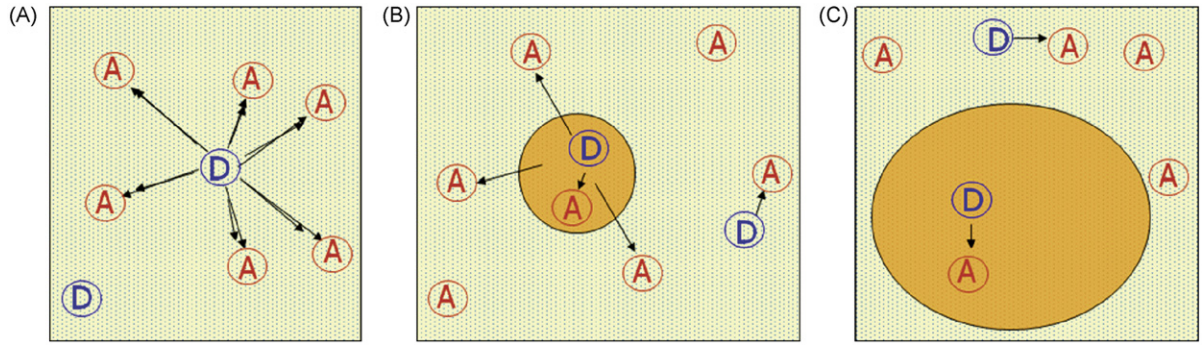

Fig. 3. Pictorial view of FRET between donor and acceptor preferring different phases in situation of: (A) no phase separation (random distribution); (B) phase separation with small domains; (C) phase separation with large domains (infinite phase separation limit, no boundary effects).

Engelborghs (1998), and an application to a peptide in a membrane is shown in the study by de Almeida et al. (2004; see Section 3.3).

Regarding the static components that can be present in the steady-state data, the first step is to consider a sphere of action, which accounts for the statistical pairs existing at the moment of excitation. From the time-resolved linear Stern–Volmer plot (Eq. (8)), and the fitting of Eq. (9) to the steady-state data I_0/I, the sphere-of-action volume V is obtained,

$$\frac{I_0}{I} = \left(\frac{\bar{\tau}_0}{\bar{\tau}}\right) \exp(-VN_A[Q]) \quad (9)$$

where N_A is the Avogadro's number.

In case that the sphere radius recovered is greater than the sum of the collisional radii of fluorophore and quencher (~10 Å for typical molecular pairs), a model considering the formation of a molecular complex should be invoked. The expression for the case where the equilibrium constant is not very high, or the quencher concentration is low, is given by Castanho and Prieto (1998).

The self-quenching mechanism is less used to obtain structural information. However, this is a very common interaction in membrane studies, due to the compartmentalization effect, that leads to high effective concentrations of molecules in a membrane, and is frequently on the origin of variations of probe lifetime with concentration or lipid phase.

When studying dynamic self-quenching, the Stern–Volmer relationship (Eq. (8)) holds, where now the quencher concentration [Q], is replaced by the fluorophore concentration [F], and the value of $\bar{\tau}_0$ is the value for very low fluorophore concentration, at which there is no self-quenching. However, the same is not valid for the steady-state data, because the total intensity becomes higher due to the increase in fluorophore, but there is a concomitant decrease due to the self-quenching interaction. This leads to the following hyperbolic type relationship,

$$I_F = \frac{C[F]}{1/\bar{\tau}_0 + k_q[F]} \exp(-VN_A[F]) \quad (10)$$

where I_F is the fluorescence intensity and C a constant.

The above formalisms assumed that diffusion in the membrane happens in three-dimensions. The solution for a bidimensional system (Razi-Naqvi, 1974) when applied to a membrane is relevant in case that the fluorescence lifetime was in order of hundreds of nanoseconds, which is not the case for most probes.

2.4. Microscopic fluorescence decays, FLIM and membrane labelling

The use of fluorescence microscopes with the ability of optical sectioning, either confocal microscopes or two-photon microscopes, that are at the same time laser scanning microscopes is nowadays a common feature in many labs (Conchello and Lichtman, 2005). In those fluorescence microscopes, if both the excitation source and the detection components fulfil the requirements for time-resolved measurements described in Section 2.1, it is possible to obtain microscopic time-resolved fluorescence decays. Both the time-domain and the frequency domain methods are possible. Obtaining fluorescence lifetimes by the frequency domain can be much faster, which can be an advantage for obtaining 3D fluorescence lifetime images. Also, it is suggested that with this method some artefacts are easier to rule out, as for example, the contribution of bleaching components for the fluorescence decay (Dong et al., 1998). Time-domain lifetime measurements can be performed by gated image intensifiers or charge-coupled devices (CCDs), by counting the photons in several parallel time gates or by time correlated photon counting (Becker et al., 2004b). This method has the main advantage of high counting efficiency, but also the detection time-resolution and speed of acquisition have been increasing (Becker et al., 2004a). The performance of each kind of system has been tested and described elsewhere (Gratton et al., 2003).

It is possible to perform three different types of time-resolved fluorescence experiments to characterize lipid heterogeneity. In the classical cuvette experiment, the ensemble average of the sample is studied, and decays with several thousands of photons in the peak channel and a large number of channels are obtained. These decays have the advantages already explained in Section 2.1. Photobleaching is a minor problem because the molecules in the excitation volume are constantly being replenished. Under the microscope, two types of experiments can be carried out. A specific microscopic region of interest smaller then the usual region of observation is selected by the user and decays with a large number of counts can be obtained (also called single point measurement; Ariola et al., 2006). In this kind of experiment, it is possible to detect complex behaviour, but the decay does not have to match the cuvette decay. Photobleaching can be a problem, and fluorescence may fade out even before the required number of counts has been accumulated. The other type of experiment is the FLIM. In this case, the x–y scan is made at the same time that the fluorescence decay is collected for each pixel, providing spatial resolution of the fluorescence lifetime and this information is invaluable in lipid domain studies. In the FLIM measurements, a small number of photons per pixel are collected, which makes it difficult to distinguish multi-exponentials. Many times a binning procedure has to be applied, and the effective resolution is in fact lower than the optical resolution of the microscope. In addition, the number of pixels may have to be much lower than the one usually used for steady-state imaging, and the resulting image has a "pixelized" look. This can be smoothed by performing pixel interpolation. Recently, new approaches to FLIM data analysis have been proposed, that avoid problems of the multi-exponential analysis in FLIM images, and that can be applied both to time-domain and frequency-domain data (Digman et al., 2008). One important difference between the FLIM vs. the cuvette or the single-point microscopic experiments is the time resolution. In FLIM, usually only 64 time channels are used (again, a consequence of the small number of photons), whereas in the other types of experiment, usually 1024 (or even 4096) channels can be used, i.e. the time resolution is 16 or more times better. One may say that it is a compromise between time and spatial resolution.

Most lipids do not display intrinsic fluorescence, thus the application of fluorescence spectroscopy to this kind of studies requires the labelling of the bilayer with an extrinsic fluorophore (membrane probe). Membrane probes include fluorescent molecules similar to natural lipids. 1,6-Diphenyl-1,3,5-hexatriene (DPH) and their derivatives having the same chromophore, such as the cationic trimethylamino-DPH (TMA-DPH), are most widely used. The structure, fluorescence properties, and applications of DPH and DPH derivatives were reviewed by Lentz (1988; see also Lentz and Burgess, 1989). Important information about the membrane can be obtained using linear conjugated polyene fluorescent fatty acids such as all-*trans*-9,11,13,15-octadecatetraenoic acid, known as *trans*-parinaric acid (*t*-PnA) and all-*trans*-8,10,12,14,16-octadecapentaenoic acid (Wolber and Hudson, 1982; Mateo et al., 1996). Fluorescence properties of *t*-PnA and *t*-PnA-containing lipids were reviewed by Hudson and Cavalier (1988). These probes are very suitable for cuvette experiments, and examples will be given along this article. However, due to both excitation and emission on the UV, they are not useful for optical microscopy. The exceptions are the pentaene chromophores, which have emission in the visible and have been used to follow different lipid species in live mammalian cells (Kuerschner et al., 2005; Van Meer and Liskamp, 2005). Finally, an important class of lipid analogue probes are sterol analogues, for which the sterols with conjugated unsaturated dou-

ble bonds are the ones with a structure and membrane behaviour that most resemble those of the sterol they are intended to mimic, whereas sterols labelled with an extrinsic fluorophore often behave in a markedly different manner (e.g. Loura et al., 2001b). For a review, see Wustner (2007).

Lipid phase separation and behaviour have been addressed with the probe laurdan (6-dodecanoyl-2-dimethylaminonaphtalene) through the determination of fluorescence lifetimes (Mukherjee and Chattopadhyay, 2005), but it is a common probe also in two-photon microscopy (e.g. Dietrich et al., 2001). Another important class of fluorescent membrane lipid analogues are cyanine dyes. They are amphiphilic molecules, with a "headgroup"—located fluorophore, and two acyl chains. Depending on the acyl chains, they prefer different lipid phases. The variety of headgroups corresponds to a large diversity of excitation and emission wavelengths, molar absorption coefficients and quantum yields. The fluorescence lifetime of these probes also depends on the lipid phase (Loura et al., 2000; Wolf, 1988). Probes of this family have been used recently in several fluorescence confocal microscopy and fluorescence correlation spectroscopy studies of lipid heterogeneity (Korlach et al., 1999; Scherfeld et al., 2003). In addition to these, there is a wide range of acyl chains or phospholipid tails and headgroups attached to well known fluorophores (Rhodamine, BODIPY, etc.).

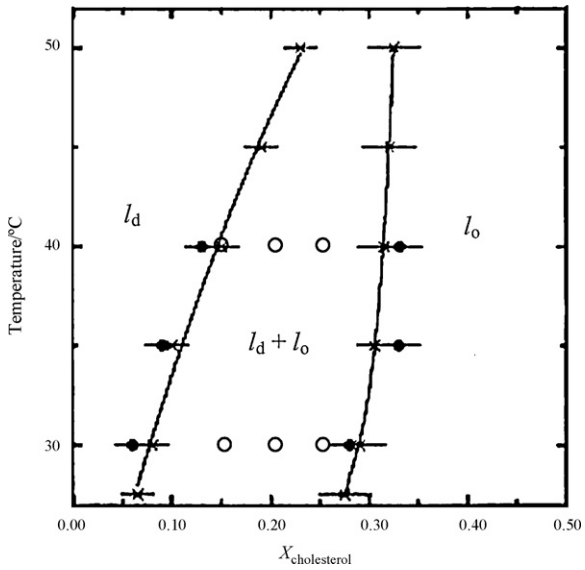

Fig. 4. DMPC/Chol phase diagram above the T_m of DMPC: l_d/l_o phase coexistence boundaries, from fluorescence recovery after photobleaching (×) (Almeida et al., 1992), and from *t*-PnA fluorescence lifetime distribution data (●) (Mateo et al., 1995); inside the phase coexistence region the (temperature, composition) points studied by FRET of the Förster pair NBD-DMPE/Rhodamine-DMPE are indicated (Loura et al., 2001c).

3. Applications

3.1. Cholesterol-induced domains and rafts

A group of lipid mixtures that have been intensely studied are phospholipid (mainly phosphatidylcholine (PC))/Chol binary systems. The well-known effects of Chol on the bilayer properties (see, e.g. Ipsen et al., 1990; Needham and Nunn, 1990) have been rationalized considering that in the presence of high amounts of Chol in a PC bilayer, the membrane is in a liquid ordered (l_o) phase (using the nomenclature introduced by Ipsen et al., 1987) with properties midway between the gel and the fluid. In this nomenclature, the gel and fluid phases are designated by solid ordered (s_o) and liquid disordered (l_d), respectively. The phase diagram is monotectic and for intermediate Chol concentrations phase coexistence occurs: s_o and l_o, below the monotectic temperature (which is close to T_m) and l_d with l_o, above the monotectic temperature. Several models have been proposed to describe PC/Chol interactions, and some of them preclude the l_d/l_o phase separation (others also rule out s_o/l_o coexistence). In other cases (Lentz et al., 1980; McMullen and McElhaney, 1995) the system is described by more complex phase diagrams, exhibiting multiple phase coexistence regions; see also Sabatini et al. (2008) for phospholipid/sterol monolayer properties. However, in the framework of this review, the typical model with a monotectic phase diagram, such as those published for the more usual and relevant PC/sterol mixtures is considered (1,2-dipalmitoyl-*sn*-glycero-3-phosphocholine (DPPC)/Chol (Ipsen et al., 1987; Vist and Davis, 1990; Sankaram and Thompson, 1991; de Lange et al., 2007; Chiang et al., 2007); 1,2-dimyristoyl-*sn*-glycero-3-phosphocholine (DMPC)/Chol (Almeida et al., 1992; Mateo et al., 1995), DPPC/ergosterol (Hsueh et al., 2005), DPPC/stigamsterol (Wu et al., 2006), 1-palmitoyl,2-oleoyl-*sn*-glycero-3-phosphocholine (POPC)/Chol at low temperatures (Thewalt and Bloom, 1992), sphingomyelin (SM)/Chol (Sankaram and Thompson, 1990; de Almeida et al., 2003; Collado et al., 2005; Arsov and Quaroni, 2008) and coexistence of two liquid phases above T_m of POPC mixed with either ergosterol or Chol (Mateo et al., 1995; de Almeida et al., 2003; Silva et al., 2006a; Hsueh et al., 2007).

To obtain the l_d/l_o phase coexistence boundaries in the mixture DMPC/Chol, a method based on the fluorescence lifetime distribution of *t*-PnA obtained by the maximum entropy method was applied (Mateo et al., 1995). In the study by Mateo et al., a Chol-induced long component in the lifetime distribution of *t*-PnA in DMPC vesicles was apparent. The amplitude of this component was constant up to ~5 mol% Chol and increased thereafter, reaching a maximum value for ~30 mol% Chol. These Chol mole fraction values are just slightly higher than the phase boundaries of the phase diagram previously obtained by fluorescence recovery methods (Almeida et al., 1992), validating the use of *t*-PnA lifetime distribution to obtain l_d/l_o phase coexistence boundaries (Mateo et al., 1995; see Fig. 4). Steady-state and time-resolved emission spectra of an *sn*-2,5-dimethylamino-1-naphthalenesulfonyl)amino (or DANSYL)-labelled PC also suggest that phase separation persists for Chol mole fractions higher than 0.3 at 30 °C when mixed with DMPC (see Troup and Wrenn, 2004, and references therein).

Other studies were aimed to probe domain size using time-resolved FRET. In one of them (Loura et al., 2001c), *N*-(7-nitrobenz-2-oxa-1,3-diazol-4-yl)-dimyristoylphosphatidylethanolamine (NBD-DMPE) and *N*-(lissamine Rhodamine B sulfonyl)-dimyristoylphosphatidylethanolamine (Rhodamine-DMPE) were used as donor and acceptor, respectively. The two headgroup-labelled phospholipid analogs have distinct distributions between the two phases, with Rhodamine-DMPE preferring the l_d phase (see Table 1) and NBD-DMPE preferring the l_o phase (see Fig. 2 for analogue probes *N*-NBD-dipalmitoylphosphatidylethanolamine (NBD-DPPE) and *N*-Rhodamine-dioleoylphosphatidylethanolamine (Rhodamine-DOPE) in another l_d/l_o coexistence system). Accordingly, FRET efficiency decreases as a consequence of phase separation. For low Chol fraction, the experimental value of acceptor concentration in the disordered phase, recovered from direct application of the FRET model to the global analysis of the fluorescence decays, is smaller than that calculated from the partition coefficient and lever rule. These findings indicate that donors located in one phase are able to make FRET to acceptors in the other phase (Fig. 3B). Together with numerical simulations of fluorescence decays, this suggests that in that region of the phase diagram, the l_o domains, dispersed

in l_d phase, should be very small (of the order of magnitude of R_0, that is, a few nm). This is not observed for higher Chol mole fractions, and domains of l_d in the Chol-rich end of the coexistence range have comparatively large size.

Although not the most intensely studied, the mixture POPC/Chol is particularly relevant. In fact, POPC is a 1-saturated, 2-unsaturated PC, a common motif found in naturally occurring phospholipids, being the major lipid component in PC isolated from several natural sources (Marsh, 1990). It has a low T_m (Koynova and Caffrey, 1998) but it has the ability to form a l_o phase in the presence of Chol both below (Thewalt and Bloom, 1992) and above (Mateo et al., 1995) T_m, i.e., s_o/l_o and l_d/l_o phase coexistence, respectively. Following the above mentioned partial determination of the phase diagram DMPC/Chol from the lifetime distribution of *t*-PnA (Mateo et al., 1995), the same method was used to obtain the l_d/l_o coexistence region for POPC/Chol, as again the existence of l_o phase also induces the presence of a long lifetime component of *t*-PnA in POPC vesicles (see also Table 1). After determining an approximate l_o/l_d partition coefficient of the probe by an independent fluorimetric assay, the l_o/l_d phase coexistence boundaries could be determined for POPC/Chol. The most important feature was that, in opposition to saturated PC/Chol mixtures, l_d/l_o coexistence close to the physiological temperature persisted up to Chol mole fractions well above the values usually encountered in mammalian plasma membranes (Mateo et al., 1995).

The complementary nature of the two sets of probes comprising DPH (and derivatives) and *t*-PnA (and derivatives) is discussed and illustrated in the study of multibilayers of phospholipids extracted from the platelet plasma membrane, with different Chol/phospholipid ratios obtained through artificial addition or removal of Chol (Velez et al., 1995; it will also be shown in the next section, for the particular case of ceramide domains).

In another recent study, the fluorescence anisotropy decay and fluorescence lifetime distribution of TMA-DPH was analysed in model membranes in the s_o, l_o and l_d phases (Sinha et al., 2003). From these results, the authors could establish criteria to identify those lipid phases, and semi-quantitatively apply them to more complex systems (namely detergent-resistant membranes and enriched-plasma membrane and its lipid extract reconstituted liposomes from human malignant glioma cells), where they detected and estimated the approximate fraction of coexisting l_o and l_d phases.

Though the lifetime of DPH does not show a remarkable dependence on the lipid phase, the modest changes observed are significant and relevant information has been taken from them. For example, the differential effects of Chol and dehydroergosterol on both fluid (POPC) and gel (DPPC) lipid bilayers at room temperature have been demonstrated (Arora et al., 2004).

The simplest model for rafts is a mixture of a high transition temperature (T_m) lipid (usually a saturated PC or SM) with a low T_m lipid and Chol (see below). The rafts would correspond to the l_o domains high T_m lipid- and Chol-enriched, in a l_d low T_m lipid-enriched matrix. The determination of a thermodynamically consistent phase diagram for the ternary mixture *N*-palmitoyl-SM (PSM)/POPC/Chol, and of the tie-line containing the equimolar mixture (Fig. 5, right), was carried out (de Almeida et al., 2003). The gel/fluid coexistence range of POPC/PSM was determined from the temperature variation of the steady-state anisotropy of DPH; the l_d/l_o coexistence for low PSM fractions (i.e. near the POPC/Chol side of the Gibbs triangle) was determined using both the fluorescence decay of *t*-PnA, and the steady-state anisotropy of DPH (see also the *t*-PnA lifetime data in the POPC/Chol system in de Almeida et al., 2004); the gel/lo coexistence range for low POPC mole fraction (i.e. near the PSM/Chol side of the phase diagram the l_o/l_d (raft/non-raft) was obtained from the trend of the amplitudes of DPH fluorescence decay components, combined with a dynamic quenching assay of DPH by the 5-nitroxyl-stearic acid. From the retrieval of the same l_d/l_o boundaries from DPH anisotropy and *t*-PnA lifetime-weighted quantum yield, and a linear trend of those parameters, a l_d/l_o partition coefficient close to one was confirmed (note that this value for *t*-PnA was also determined by Mateo et al. (1995) from fluorescence anisotropy decays and maximum entropy methods (Table 1), showing that the probe can safely be used to

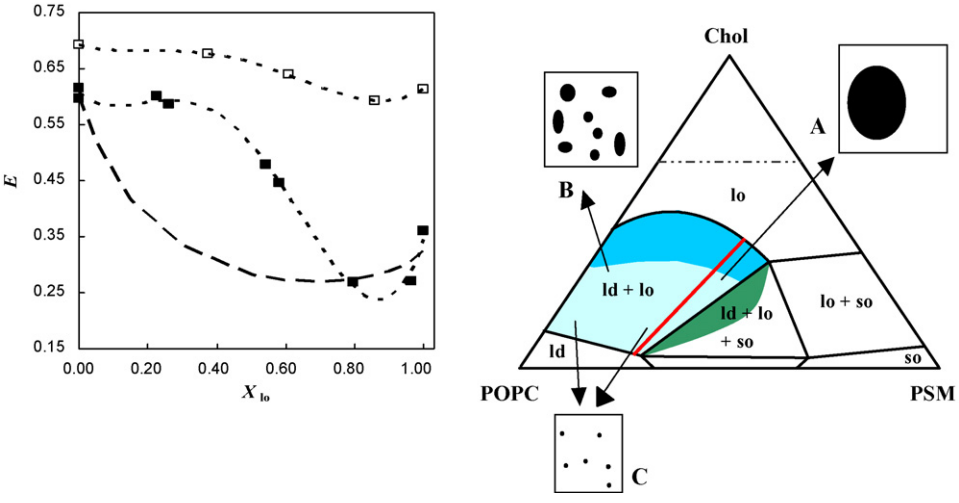

Fig. 5. Left: Variation of FRET efficiency as a function of l_o phase mole fraction between the donor/acceptor pair (a) NBD-DPPE/Rhodamine-DOPE in PSM/POPC/Chol large unilamellar vesicles, along the tie-line containing the lipid mixture 1:1:1 (mol: mol: mol) at 23 °C (red line of right panel) with 0.2 mol% of acceptor (■); (b) NBD-DMPE/Rhodamine-DOPE in DMPC/Chol, along the tie-line at 30 °C (see Fig. 4) with 0.2 mol% of acceptor (□). The dotted lines are merely guides to the eye. The theoretical line for infinite phase separation (large domains) for the ternary mixture is also shown (thick broken line). Adapted from de Almeida et al. (2005). Right: PSM/POPC/Chol phase diagram at 23 °C, showing also the boundaries and schematic illustrations of the size of lipid rafts. Rafts are present in the blue-shaded area (l_d/l_o coexistence). In the darker area, lo predominates over l_d, and the reverse occurs for the light-shaded area. Rafts can also exist in the green-shaded area, where there is coexistence of three-phases, but the so phase is present only in very low amounts. Insets: (A) region of large rafts; detected by microscopy and FRET (>75–100 nm); (B) region of intermediate size rafts: detected by FRET but not by microscopy (between ~20 nm and ~75–100 nm); (C) region of small rafts: not detected by FRET nor microscopy (<20 nm). Adapted from de Almeida et al. (2005).

determine phase boundaries in this system, and it is not biased by the method of fluorescence decay analysis). The complete diagram, shown in Fig. 5 (right) allowed a good estimation of the l_d/l_o (non-raft/raft) tie-line that contains the 1:1:1 POPC/PSM/Chol mixture (also depicted in the figure), and the direction of the tie-line was further confirmed by measuring the *t*-PnA fluorescence lifetime and DPH anisotropy in those mixtures, which behaviour was similar to the one observed for low or zero PSM mole fraction, thus showing internal consistency of the methods employed. The phase behaviour of this and very similar mixtures was later confirmed, and extended to other temperature and pressure ranges by a variety of techniques (e.g. Nicolini et al., 2006a,b; Coste et al., 2006; McQuaw et al., 2007; Bunge et al., 2008; Halling et al., 2008).

In this way, partition coefficients of other fluorescent probes (see Table 1) and FRET efficiency along the tie-line could be determined, and information on the rafts' size was obtained (de Almeida et al., 2005). As a FRET pair, the probes NBD-DPPE and Rhodamine-DOPE were used. In Fig. 2 the lifetime quantum yield of the probes as a function of l_o mole fraction is shown, together with the fit of Eq. (5), showing the preference of NBD-DPPE for the l_o phase, and of Rhodamine-DOPE for the l_d phase. In Fig. 5 (left), the experimental FRET efficiency is presented, together with the value predicted for very large domains. This one presents a parabolic shape, whereas the experimental curve is more complex, pointing to alterations on the size of the domains along the tie-line. For very low l_o fractions, the l_o domains are very small (below 20 nm), and increase with increasing l_o mole fraction (de Almeida et al., 2005). For very large l_o fraction, the experimental FRET efficiency value approaches that of infinite domains (which for the used FRET pair means >∼75 nm). By representing FRET efficiency as a function of l_o mole fraction one can compare different systems with l_o/l_d phase coexistence in the same plot. For example, in Fig. 5 (left), the FRET efficiency for the binary system DMPC/Chol (Loura et al., 2001c) discussed above is also shown. It can be readily observed that the decrease in FRET is much less pronounced than in the ternary system. This points to a lower limit for the size of the domains in binary PC/Chol mixtures, and is probably the cause of the lack of detection of l_o/l_d heterogeneity in these kind of mixtures by fluorescence microscopy (Veatch and Keller, 2003), as mentioned in Section 1.

Another noteworthy feature of the time-resolved fluorescence data obtained is that the trend of variation of the lifetimes, which is independent of the domain size, for both Rhodamine and NBD probes, was the same in case of DMPC/Chol and the ternary l_d/l_o tie-lines, and in all cases could be described by Eq. (5). This shows that the fluorescence lifetimes of the probes can be used to probe the nature of lipid domains, and to determine lipid phase coexistence regions in raft-like systems, regardless of the size of the domains. The latter information can then be concluded from time-resolved FRET experiments, as explained above.

3.2. Ceramide-induced domains

Although historically the most common type of lipid heterogeneity studies involved binary lipid mixtures with gel/fluid phase separation (e.g. Marsh, 1990), the field has been evolving towards characterization of more complex systems, closer to biological membranes (Edidin, 2003). Recently, the attention on solid or gel-like lipid domains has re-emerged, due to the awareness that sphingolipids, with several roles in fundamental cellular processes, at physiological concentrations, tend to segregate forming those kinds of phases (Goñi and Alonso, 2006). Sphingolipids play also an essential role in maintaining bilayer stability and in the formation of lipid rafts (Simons and Van Meer, 1988; Degroote et al., 2004).

Ceramide (Cer) is the cellular precursor of SM, and can also be formed from SM at the cell surface, through the action of the enzyme sphingomyelinase (SMase), with marked effects on rafts and cell processes such as signal transduction (e.g. Bezombes et al., 2004). Numerous studies show that ceramide production in response to external stress stimuli is a nearly universal feature of programmed cell death (for reviews see Mathias et al., 1998; Ruvolo, 2003). Evidence is emerging for the indirect action of ceramide, resulting from the alterations of the biophysical properties of the plasma membrane (Kolesnick et al., 2000; Cremesti et al., 2002). To understand the role of ceramide in signal initiation and lipid second-messenger formation from rafts, it is necessary to systematically characterize the changes that occur at the plasma membrane upon increasing ceramide levels.

In order to address these aspects, the effect of increasing amounts of *N*-palmitoyl-ceramide (PCer) on the properties of POPC bilayers was systematically studied (Silva et al., 2006b). Three probes with different lipid-phase related properties were employed (Table 1): *t*-PnA which partitions preferentially to gel phases (Mateo et al., 1993a; de Almeida et al., 2002); DPH, which is expected to distribute equally between phases (Lentz, 1988; Davenport, 1997); and *N*-(7-nitrobenz-2-oxa-1,3-diazol-4-yl)-dioleoyl-PE (NBD-DOPE), a phospholipid with unsaturated acyl chains and the fluorescent label in the headgroup, preferring fluid rather than gel lipid phases (Vaz and Melo, 2002). Comparing the behaviour of the probes (Silva et al., 2006b), it can be concluded that whilst *t*-PnA partitions to PCer-gel domains and thus is able to follow PCer domain formation and report their properties, DPH is excluded from these domains. Moreover, regarding that usually the partition coefficient is K_p ∼1 for DPH in a typical gel-fluid separation, the ceramide-rich gel domains should be highly ordered and compact, in order to exclude the probe. As a consequence, DPH reports only the properties of the fluid POPC phase. On another hand, the head-labelled lipid NBD-DOPE is the only probe among those three that is able to detect a transition of one type of PCer gel to another type of an even more ordered gel, where dehydration and increased rigidity at the headgroup membrane/water interface level occurs. The building-up of a complete POPC/PCer phase diagram was only possible after an exhaustive characterization of the fluorescence properties of the three probes as a function of temperature and composition. After the phase diagram determination, the FRET method along a tie-line described in the previous section could be applied. In the present case FRET from *t*-PnA to NBD-DOPE showed that the ceramide-rich domains reach the infinite phase separation value readily (Silva et al., 2006b).

To better understand how ceramide modulates the biophysical properties of the membrane, the interactions between PCer and PSM were studied in the presence of POPC in membrane model systems (Castro et al., 2007). This system (Fig. 1) can mimic the lipid composition of the organelle membrane where SM synthesis occurs from Cer, or the changes that occur in the plasma membrane upon SMase action following an apoptotic stimulus. The previous characterization of the binary POPC/PCer system (Silva et al., 2006b), and the opposite behaviour of *t*-PnA and DPH, with one preferring and the other being excluded from PCer gel domains were instrumental to the study of the ternary system (Fig. 1). In these mixtures, PCer recruits POPC and PSM in the fluid phase to form extremely ordered and compact gel domains that exclude DPH. Gel domain formation by low PCer mol fraction (up to 12 mol%) is enhanced by physiological PSM levels (20–30 mol% total lipid). For higher PSM content, a three-phase situation, consisting of fluid (POPC-rich)/gel (PSM-rich)/gel (PCer-rich) coexistence, is clearly shown, because the steady-state anisotropy of DPH increases linearly with PSM fraction (gel/fluid partition coefficient close to 1), but actually decreases when PSM is replaced by PCer (exclusion from the new gel). Simultaneously, *t*-PnA average lifetime abruptly increases with the presence of small amounts of PCer (higher K_p PCer/POPC

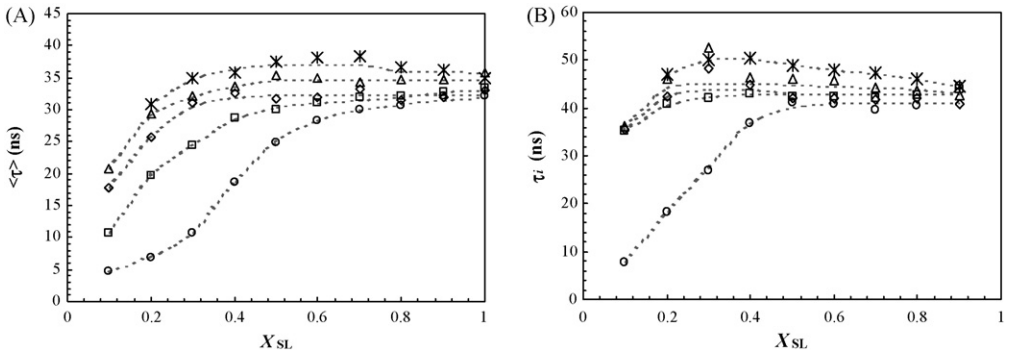

Fig. 6. Effect of PCer on *t*-PnA's mean fluorescence lifetime (<τ>) (panel A) and fluorescence lifetime of the long component of *t*-PnA fluorescence decay (panel B) in POPC/PSM mixtures containing 0 (○), 2 (□), 4 (◊), 8 (△) and 12 (*) mol% PCer, as a function of total sphingolipids mole fraction ($X_{SL} = X_{PSM} + X_{PCer}$). The dashed lines are merely a guide to the eye. A long component longer than 30 ns is unequivocal evidence for the presence of gel phase. Adapted from Castro et al. (2007).

than PSM/POPC), as shown in Fig. 6A. In Fig. 6B, the long component of *t*-PnA fluorescence decay confirms that that increase is due to the formation of a new gel phase that excludes DPH and explains why the fluorescence lifetime of *t*-PnA is so sensitive to its presence. To determine the fraction of each phase a quantitative method was developed, taking into account the K_p of the probes between PCer-rich/POPC-rich and PSM-rich/POPC-rich phases, and the fluorescence parameters of the probes in each phase. This allowed establishing the complete ternary phase diagram through an iterative method (Fig. 1), which helps to predict PCer-rich gel domain formation (e.g. upon SMase action) and explains its enhancement through PSM/PCer interactions. It also shows that the Cer-rich gel can incorporate ~30 mol% of the otherwise fluid POPC. The extrapolation of the phase coexistence boundaries to high total sphingolipid content (low POPC mole fraction) led to the conclusion of existence of PCer/PSM gel/gel phase separation, in agreement with recently observed gel/gel phase separation by fluorescence microscopy for the binary mixture egg SM/egg Cer (Sot et al., 2006).

As previously mentioned and shown in Table 1, *t*-PnA has a K_p of ~1 between l_d and l_o in the ternary raft system POPC/PSM/Chol, in the tie-line containing the 1:1:1 mixture. In addition, the decay of *t*-PnA fluorescence shows a long component (>30 ns) in PCer rich gel that is absent in both l_d and l_o phases along the mentioned tie-line. This allowed using the fluorescence lifetime of *t*-PnA in the ternary system contaminated with physiological amounts of PCer (up to 4 mol%) to quantify the formation of PCer rich gel (Silva et al., 2007). This gel phase, again excluding DPH, was not composed solely of PCer, because the fraction of gel formed was higher than the fraction of PCer added to the system. The gel was mainly formed in the region of the raft ternary tie-line where low lo fraction is present (the small raft-size region), and is abolished for higher lo fraction (large raft size). Time-resolved FRET experiments also showed that PCer was not able to induce the coalescence of small rafts (FRET between NBD-DPPE and Rhod-DOPE), that PCer domains were also small (~4 nm; FRET between *t*-PnA and NBD-DOPE), and that PCer gel domains were in average closer to the rafts than to the disordered domains (FRET between *t*-PnA and NBD-DPPE) (Silva et al., 2007).

3.3. Protein-induced domains

Dynamic quenching and time-resolved FRET have proved to be valuable tools in the study of lipid–protein interaction, and this section focuses on recent applications to protein-(or peptide-)induced membrane reorganization studies, where domain formation was investigated. Several experimental set-ups can be used in lipid-protein studies, and this section exemplifies them with recent applications.

Commonly, in a FRET experiment the donor is the protein/peptide under study (either wild-type, if it has fluorescent residues, or labelled with a convenient fluorophore), and the acceptors are membrane probes. Although this set-up is most convenient for the study of lipid selectivity around the protein (Fernandes et al., 2004), it can also be used to probe eventual protein-induced phase separation. In the latter situation, the experimental donor decay in presence of acceptor (or the extent of FRET) is analyzed using the theoretical equations for uniform acceptor distribution. Successful analysis with recovery of the correct acceptor concentration is evidence for uniform distribution of acceptor around the protein, and therefore lack of protein-induced phase separation. Enhanced FRET is indicative of preferential protein-acceptor probe association, or phase separation with co-localization of protein and acceptor probe.

A recent study involved acetyl-GWW(LA)8LWWA-amide (WALP23), a transmembrane model peptide with flanking tryptophans, incorporated in fluid DMPC bilayers containing variable amounts of Chol analog dehydroergosterol (DHE), a suitable FRET acceptor to tryptophan, as well as equal amounts of Chol in control experiments (Holt et al., 2008). The aim was to investigate how tryptophan and Chol interact with each other and what the possible consequences were for membrane organization, following literature reports of a possible preferential interaction between Chol and tryptophan residues located near the membrane–water interface (Gasset et al., 1988; Santiago et al., 2001; Carozzi et al., 2002; Van Duyl et al., 2005). It was found that WALP23 fluorescence decays in presence of DHE, both with and without added equimolar amounts of Chol, could be satisfactorily globally analyzed assuming uniform DHE distribution in the bilayer. These results agree with ^{2}H NMR quadrupolar splitting measurements and point to the absence of evidence for a preferential interaction between Chol and tryptophans located at the bilayer interface.

The FRET pair Trp/DHE had been used in a similar manner previously (de Almeida et al., 2004) in a study of the hypothetical affinity of the γM4 peptide from the muscle acetylcholine receptor (donor: Trp^{453}) for Chol (acceptor: DHE) in the l_o phase of POPC/Chol. It was found that the measured FRET efficiency was significantly lower than expected, and the data could only be rationalized with an effective sterol concentration ~38% lower than the analytical expected concentration. It is argued that this is the result of reduction in the area available for the dispersion of sterol caused by the formation of peptide rich-patches. This agrees with the observed dynamic self-quenching of γM4 fluorescence. The same degree of quenching is obtained for 7 mol% peptide in l_d and for all concentra-

tions in l_o. Since the diffusion coefficient in l_o is threefold lower than in l_d (e.g. Dietrich et al., 2001), it can be assumed that the effective concentration of peptide is threefold higher in the patches. Using the area per lipid molecule for the l_o phase, it can be concluded that the γM4 peptide occupies ~30% of the area in the patches in agreement with the FRET data.

Another possible experimental design is using protein/peptide labelled with a donor fluorophore, and the same protein/peptide labelled with an acceptor chromophore. Although this set-up is especially useful to probe eventual protein oligomerization (Adair and Engelman, 1994; Li et al., 1999), in case that this phenomenon can be ruled out from independent experiments, then enhanced FRET can be attributed to phase separation with preferential protein partition to one of the phases. This approach is exemplified by a study of the lateral distribution and oligomerization properties of M13 bacteriophage major coat protein in membrane model systems (Fernandes et al., 2003).

Arguably, the most appropriate experimental FRET design to study eventual protein/peptide-induced heterogeneity is the use of both donor and acceptor membrane probes. It is easy to check that in the absence of protein there are (no) pre-formed domains, and protein oligomerization does not hamper the FRET analysis. Enhanced FRET between donor and acceptor which mimic the same lipid species, or reduced FRET between donor and acceptor which mimic different components of the lipid mixture can therefore in principle be ascribed to protein/peptide-induced phase separation.

This was the rationale behind our recent study of the effect of a model basic peptide, hexalysiltryptophan (K_6W), on the organization of the zwitterionic/anionic lipid mixture DPPC/dipalmitoylphosphatidylserine (DPPS) (Loura et al., 2006). To this extent, two fluorescent PC analogues were used as a FRET pair (DPH-PC, donor; NBD-PC, acceptor). Two distinct situations were considered: at $T = 60\,^{\circ}C$, above the main transition temperature (T_m) of both phospholipids, there is a single fluid lipid phase in the

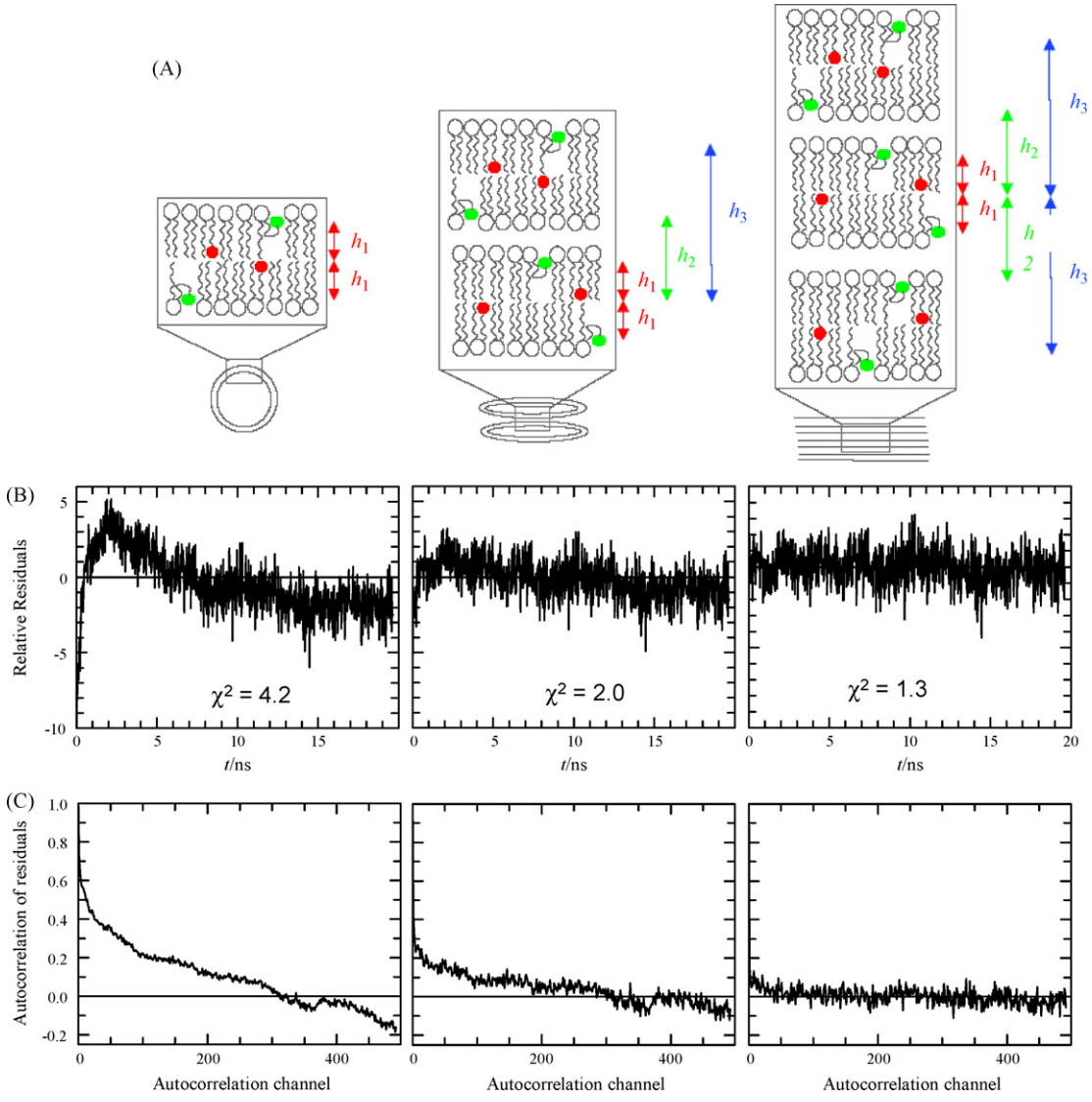

Fig. 7. Membrane rearrangement induced by the peptide K_6W in DPPC:DPPS membranes studied by time-resolved FRET between donor DPH-PC (red labeled lipid) and acceptor NBD-PC (green labeled lipid). Residuals (B) and autocorrelation of residuals (C) of the fits to the fluorescence decay of DPH-PC, NBD-PC:total lipid = 1:250, [K_6W]= 100 μM, DPPC:DPPS 1:1 (mol:mol) vesicles at 60 °C. Total lipid concentration was 0.75 mM. The models used were, from left to right, in both panels: bilayer geometry (panel A, left), bilamellar geometry (panel A, centre) and multibilayer geometry (panel A, right). The symbols h_n represent the inter-plane distances considered in each model. Adapted from Loura et al. (2006).

absence of peptide; at $T = 45\,^{\circ}C$, between the T_m values for DPPC and DPPS, there is gel/fluid phase coexistence in the absence of peptide. The addition of this basic peptide could in principle lead to: (i) phase separation from a single fluid phase DPPC/DPPS mixture ($T = 60\,^{\circ}C$) and, (ii) noticeable reorganization of pre-existing gel/fluid domains ($T = 45\,^{\circ}C$). The former effect would be clearly apparent in a FRET measurement, as segregation of a DPPC-rich phase (containing most of the probe molecules) would lead to local enrichment of acceptor probe, and thus higher FRET efficiency. The latter effect would be visible for example if the pre-existing domains were very small (~10 nm or smaller), and became considerably larger upon incorporation of peptide (Fig. 3). The main conclusions are: (i) at 45 °C, addition of peptide does not lead to appreciable changes in domain organization, which are already large (in FRET terms); (ii) at 60 °C, there is an increase in FRET efficiency upon addition of peptide, but this is caused by vesicle aggregation rather than phase separation, as revealed by analyzing the time-resolved data with the respective model decay laws. It was necessary to consider FRET to other planes containing acceptors (due to bilayer stacking) to obtain satisfactory analysis of the donor fluorescence decay (Fig. 7). A multibilayer geometry is formed (with K_6W molecules bridging adjacent lipid bilayers), and a limit lamellar repeat distance of ~57 Å was recovered. Furthermore, no evidence for lateral domain formation on the FRET length scale was found at this temperature, the cationic peptide being only able to induce local lipid demixing, causing a short-range sequestration of 2–3 acidic lipids around each surface-adsorbed peptide.

3.4. FLIM studies of membrane lipid domains and rafts

FLIM has only very recently started to be applied to the study of lipid phases in membrane model systems (see below). However, there were already studies concerning raft-related protein interactions where FRET-FLIM was used in cell membranes. The raft dependent interaction of tetanus neurotoxin with Thy-1 was studied by FRET-FLIM using the frequency domain method (Herreros et al., 2001). Time-domain was used to demonstrate interaction between BACE (β site of amyloid precursor protein-cleaving enzyme) and the low-density lipoprotein receptor-related protein occurring on lipid rafts at the cell surface (Von Arnim et al., 2005). FRET microscopy on the study of lipid rafts in vivo has recently been reviewed, showing the importance of the use of non-invasive biophysical techniques, namely, combining imaging and spectroscopic principles, to study functional assemblies on the cell membrane which formation is based on lipid–lipid interactions (Rao and Mayor, 2005). The study of membrane lipid microdomains using diverse optical techniques was also recently reviewed (Owen et al., 2007).

In general, there can be some heterogeneity in the fluorescence lifetime obtained for the donor protein in the absence of acceptor, i.e. a histogram of pixel distribution of lifetimes around a value that is taken as the lifetime of the donor protein. This distribution contains itself information on the heterogeneity of the protein environment, but it can be difficult to distinguish it from the variability intrinsic to the technique, given that in each pixel the number of photons collected is quite low. The statistical uncertainty in the lifetime is higher than in a typical cuvette experiment, thus the origin of the variability that is beyond that uncertainty is not easy to ascribe (it can be either due to a different lipid environment, but also to different conformations, different states of aggregation, etc. – see previous section). In this way, the introduction of lipid membrane probes is fundamental, because their behaviour can be easily characterized in well-defined membrane model systems, and the variation in the fluorescence lifetime can be safely assigned to changes in the lipid environment. For example, Ariola et al. (2006) studied the microscopic fluorescence decays of an acyl-chain BODIPY-labelled phospholipid probe in giant unilamellar vesicles (GUVs) composed of either a single fluid (DOPC) or a single gel (DPPC) phase. They found a significant shorter average fluorescence lifetime of the probe in the gel (bi-exponential decay) as compared to the fluid phase (mono-exponential decay), and also a greater variability of the parameters describing the decay in the gel phase, both in FLIM and single point experiments. The probe:lipid ratio used, probably due to the acyl-chain position of the fluorophore which is difficult to accommodate in the tightly packed gel phase, gives raise to heterogeneity in the one component DPPC GUV. The advantage relative to a head-labelled lipid is a less marked photo-selection effect in the fluid phase. Simultaneously, Chol-rich domains in individual mast cells and the influence of extensive IgE cross-linking in the cold were investigated using the time-resolved fluorescence microscopy of Alexa 488 labelled IgE and the membrane probe $DiIC_{18}$ (Davey et al., 2007). This harsh cross-linking protocol was deliberately used in order to observe strong changes in membrane domain organization, and easily correlate their effects with the time-resolved parameters, paving the way to the study of more subtle effects. The authors found that the increased fluorescence intensity observed at cross-linked induced patches of both the Alexa-488-protein linked and the $DiIC_{18}$ cyanine membrane probe was not only a concentration effect, but definitely result of an increased quantum yield of the fluorophores, as revealed by their increased average lifetime. In the case of the protein, it is noteworthy that this was not the typical FRET-FLIM experiment described above. However, there were significant changes observed both in the average fluorescence lifetime (from both FLIM and single point experiments), and in the lifetime distribution of the pixel histogram from the FLIM images, which became bimodal after cross-linking. These changes were certainly consequence of alterations in the fluorophore microenvironment, which were in their turn related to alterations in the membrane nanostructure, as probed by the $DiIC_{18}$ fluorophore.

In another recent study, a probe of the Laurdan family (see Section 2.4) named di-4-ANEPPDHQ, having a dialkyloaminonaphtalene group, was employed in a FLIM study to detect ordered membrane domains in living cells (Owen et al., 2006). The authors "calibrated" the fluorescence lifetime of the probe for different lipid phases using large unilamellar vesicle (LUV) suspensions of DOPC (fluid) and PSM:Chol 7:3 mol:mol (l_o) at 20 °C and 37 °C, and a good correlation between membrane order and the probe's lifetime was obtained. In fact, the fluorescence lifetime of the probe provided better contrast in the live epithelial cells than the spectral shift usually used, and not only increased order at the plasma membrane as compared with internal membranes was detected, but also specially ordered domains imaged in plasma membrane protrusions. They also observed a decreased lifetime (less membrane order) of di-4-ANEPPDHQ upon treatment of the cells with methyl-β-cyclodextrin or with raising the temperature from 20 °C to 37 °C.

A comprehensive study of a ternary lipid phase diagram containing l_d, l_o and s_o phases using the combination of cuvette, FLIM and single point microscopic decays was recently carried out (de Almeida et al., 2007). The system chosen was DOPC/DPPC/Chol because there were fluorescence imaging combined with NMR (Veatch et al., 2004) and confocal imaging combined with FCS (Scherfeld et al., 2003) studies in the same system, and the phase behaviour of the three binary systems DOPC/DPPC, DOPC/Chol, and DPPC/Chol (that would be the sides of the Gibbs triangle for the ternary phase diagram) was well studied (Lentz et al., 1976, 1980; Elliott et al., 2005; Ipsen et al., 1987; Vist and Davis, 1990; Veatch et al., 2006). The authors used a single probe to perform the study, because by combining the two-photon fluorescence intensity

images with the FLIM, this probe alone could identify the three lipid phases. This is because the probe, Rhod-DOPE, at the probe:lipid ratio of 1:500 used displays the same fluorescence lifetime in the gel and in the l_d phases (Table 1), but due to its unsaturated acyl chains, it prefers strongly the fluid phase, partitions mildly into the l_o phase, and it partitions much less to the gel phase, which will appear as dark regions in the intensity image (Fig. 8A). In addition, the fluorescence lifetime of the probe is severely reduced in the l_o phase (below 2 ns) as compared to the other phases (close to 3 ns), thus providing contrast in the FLIM image (Fig. 8B and C). An example of the assignment of the 3 lipid phases in one single GUV composed of DOPC/DPPC/Chol (44:44:12) mol ratio is given in Fig. 8D–F. The results were confirmed by the high-count microscopic decays, because these decays were mono-exponential in single gel or single fluid GUV, but bi-exponential with a sub-nanosecond component in gel/fluid binary GUV. In GUV with 1:1 or 7:3 DOPC/DPPC and small amounts of Chol, such decays were obtained in different regions of the GUV. In bright areas, the bi-exponential decay typical of gel/fluid coexistence was sometimes obtained, showing that the two phases are present, and that they may remain unobserved in intensity images. In addition, mono-exponential decays with a fluorescence lifetime of ~1.8 ns were obtained in other region of those GUV showing that the l_o phase was also present. The combination of all the data allowed completion of the ternary DOPC/DPPC/Chol phase diagram which contains a large l_d/l_o region and a tie triangle where l_d, l_o and s_o coexist, in addition to a gel/l_o region close to the DPPC/Chol side of the triangle (de Almeida et al., 2007). Later, a phase diagram from NMR data was obtained in the same mixture (with the exception that DPPC was chain-perdeuterated) (Veatch et al., 2007), and both phase diagrams are qualitatively very similar.

Recently, a new probe was developed that allowed FLIM detection of membrane rafts in the μm scale (upon cell activation by CD3 receptor antibody cross-linking) in Jurkat cells (Margineanu et al., 2007). This perylene monoimide derivative (PMI-COOH) offers

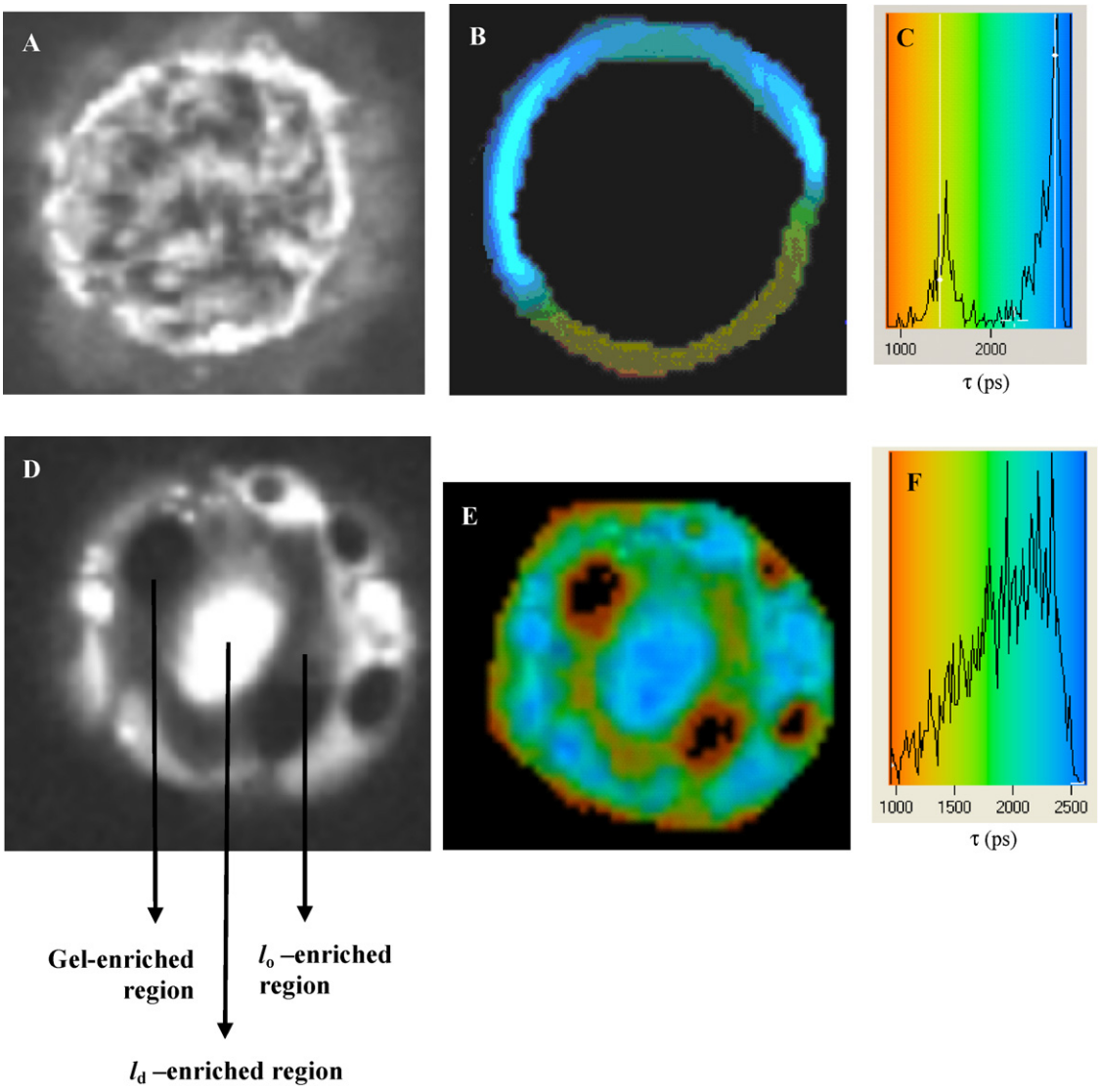

Fig. 8. Two-photon ($\lambda_{excitation}$ = 860 nm) excitation fluorescence intensity and fluorescence lifetime images of GUV pertaining to the ternary DOPC:DPPC:Chol system labelled with Rhod-DOPE (0.2 mol%), at room temperature (24 °C). (A) fluorescence intensity image of DOPC:DPPC 1:1 (mol:mol) GUV (top view) showing gel (dark)/fluid (bright) phase separation. (B) fluorescence lifetime (FLIM) image and (C) fluorescence lifetime distribution histogram of the respective FLIM image of the equatorial section of GUV composed of equimolar amounts of DOPC:DPPC:Chol. Top view fluorescence intensity image (D), fluorescence lifetime (FLIM) image (E), and fluorescence lifetime distribution histogram of the respective FLIM image (F) of a GUV composed of DOPC, DPPC, and Chol, in a 0.44:0.44:0.12 mole ratio; black spots inside the vesicle correspond to pixels with counts equivalent to the background level; in the intensity image (D), examples of regions that can be safely assigned to a certain phase behaviour based on the fluorescence lifetime of Rhod-DOPE (E) are indicated. The colour code used in the FLIM images is that indicated in the histogram to their right (adapted from de Almeida et al., 2007).

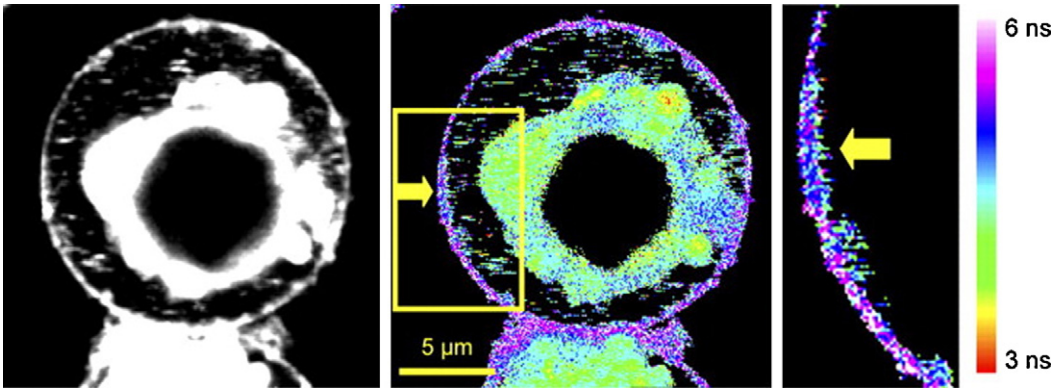

Fig. 9. Fluorescence intensity (gray) and fluorescence lifetime images (colour) obtained for PMI-COOH in Jurkat cell stimulated by cross-linking membrane CD3 receptors using specific antibodies; the yellow arrow points toward a region where the PMI-COOH lifetime is different from the rest of the membrane, which can be due to the formation of a big lipid raft. The yellow rectangle indicates the area that is magnified in the third panel (after application of a mask to the whole cell image to leave only the lifetime distribution concerning the plasma membrane) (adapted from Margineanu et al., 2007).

several advantages, such as fast incorporation into living cells, and different fluorescence decays in l_d and l_o phases (measured in small unilamellar vesicle suspensions and in GUV) which are features of probes mentioned in previous paragraphs. In addition, it is a very photostable chromophore, and has a quantum yield of ~1 in organic solvents. In this article by Margineanu et al. (2007) a comparison is made between the probes Laurdan, di-4-ANEPPDHQ and PMI-COOH, which is a useful summary of their use in the study of lipid rafts (Table 2 in that article). In Fig. 9, the fluorescence intensity image is shown for an activated Jurkat cell, together with the FLIM image. In this latter one, it can be seen that the fluorescence lifetime of the probe is much higher in the plasma membrane than in the intracellular membranes, and a domain formed upon cell activation in the plasma membrane is magnified in the right panel of the figure.

4. Conclusions

Membrane lipid domains, including the so-called lipid rafts, are a very active area of research. Although their importance is consensual, their properties are not. This stems from their dynamic and transient nature, and small size, usually below the resolution of conventional optical microscopy techniques. Thus, to obtain a full characterization of the relevant properties and role of membrane lipid domains, several techniques combined in different ways have to be used.

In this paper, it is shown how time-resolved fluorescence methods can be powerful tools in the detection and characterization of lipid domains. Time-resolved data are less prone to artifacts than steady-state fluorescence. In addition, fluorescence lifetimes contain information that in the framework of the adequate models, allows obtaining important information, such as domain size, or lipid–protein interactions. It is shown how fluorescence lifetimes allow determining probe preference (partition coefficient) between different phases, and how these parameters are essential to correctly assign lipid phase changes, or apply more complex models (e.g. in FRET studies). The variation of fluorescence lifetimes with lipid composition, also allows obtaining lipid phase diagrams, and these are instrumental in the rationalization of the behaviour of lipid mixtures.

Only very recently, time-resolved fluorescence studies with membrane probes started to be carried out under the microscope (single point microscopy decays and FLIM). The probe lifetime information obtained for the different domains that are visualized is a stronger tool as compared to the fluorescence intensity imaging methods for the assignment of the type of phases present. However, there are still limitations, namely, the acquisition time that makes photobleaching a more severe problem in time-resolved fluorescence microscopy. In the study of complex systems (e.g. co-existence of three phases), it is an advantage to combine bulk (ensemble) data obtained in cuvette work (higher time resolution and statistics), with the one from microscopy. Thus far, the examples shown of lipid domains in life cells detected by FLIM, are only in activated cells or cytoskeleton-stabilized domains, that are in the micrometer size-range. However, the development of new probes, that overcome the present limitations, will in the near future allow for the resolution of complex fluorescence decays that will contain important information about the presence and properties of membrane domains in the sub-micrometer scale.

Acknowledgment

Funding from POCI and PPCDT projects (QUI/68151/2006), FCT, Portugal, is acknowledged.

References

Adair, B.D., Engelman, D.M., 1994. Glycophorin a helical transmembrane domains dimerize in phospholipid bilayers: a resonance energy transfer study. Biochemistry 33, 5539–5544.
Almeida, P.F.F., Vaz, W.L.C., Thompson, T.E., 1992. Lateral diffusion in the liquid-phases of dimyristoylphosphatidylcholine cholesterol lipid bilayers—a free-volume analysis. Biochemistry 31, 6739–6747.
Anderson, R.G.W., Jacobson, K., 2002. Cell biology: a role for lipid shells in targeting proteins to caveolae, rafts, and other lipid domains. Science 296, 1821–1825.
Ariola, F.S., Mudaliar, D.J., Walvick, R.P., Heikal, A.A., 2006. Dynamics imaging of lipid phases and lipid–marker interactions in model biomembranes. Phys. Chem. Chem. Phys. 8, 4517–4529.
Arora, A., Raghuraman, H., Chattopadhyay, A., 2004. Influence of cholesterol and ergosterol on membrane dynamics: a fluorescence approach. Biochem. Biophys. Res. Commun. 318, 920–926.
Arsov, Z., Quaroni, L., 2008. Detection of lipid phase coexistence and lipid interactions in sphingomyelin/cholesterol membranes by ATR-FTIR spectroscopy. Biochim. Biophys. Acta 1778, 880–889.
Bagatolli, L.A., Gratton, E., 2000. Two photon fluorescence microscopy of coexisting lipid domains in giant unilamellar vesicles of binary phospholipid mixtures. Biophys. J. 78, 290–305.
Becker, W., Bergmann, A., Biscotti, G., Koening, K., Riemann, I., Kelbauskas, L., Biskup, C., 2004a. High-speed FLIM data acquisition by time-correlated single photon counting. Proc. SPIE 5323, 1–9.
Becker, W., Bergmann, A., Hink, M.A., Konig, K., Benndorf, K., Biskup, C., 2004b. Fluorescence lifetime imaging by time-correlated single-photon counting. Microsc. Res. Tech. 63, 58–66.
Bezombes, C., Grazide, S., Garret, C., Fabre, C., Quillet-Mary, A., Müller, S., Jaffrézou, J.-P., Laurent, G., 2004. Rituximab antiproliferative effect in B-lymphoma cells is associated with acid-sphingomyelinase activation in raft microdomains. Blood 104, 1166–1173.

Bretscher, M.S., Munro, S., 1993. Cholesterol and the Golgi aparatus. Science 261, 1280–1281.
Buboltz, J.T., 2007. Steady-state probe-partitioning fluorescence resonance energy transfer: a simple and robust tool for the study of membrane phase behavior. Phys. Rev. E: Stat. Nonlin. Soft Matter Phys. 76, 021903.
Bunge, A., Müller, P., Stöckl, M., Herrmann, A., Huster, D., 2008. Characterization of the ternary mixture of sphingomyelin, POPC, and cholesterol: support for an inhomogeneous lipid distribution at high temperatures. Biophys. J. 94, 2680–2690.
Carozzi, A.J., Roy, S., Morrow, I.C., Pol, A., Wyse, B., Clyde-Smith, J., Prior, I.A., Nixon, S.J., Hancock, J.F., Parton, R.G., 2002. Inhibition of lipid raft-dependent signaling by a dystrophy-associated mutant of caveolin-3. J. Biol. Chem. 277, 17944–17949.
Castanho, M.A.R.B., Prieto, M., 1998. Fluorescence quenching data interpretation in biological systems. The use of microscopic models for data analysis and interpretation of complex systems. Biochim. Biophys. Acta 1373, 1–16.
Castro, B.M., de Almeida, R.F.M., Silva, L.C., Fedorov, A., Prieto, M., 2007. Formation of ceramide/sphingomyelin gel domains in the presence of an unsaturated phospholipid: a quantitative multiprobe approach. Biophys. J. 93, 1639–1650.
Chiang, Y.-W., Costa-Filho, A.J., Freed, J.H., 2007. Dynamic molecular structure and phase diagram of DPPC-cholesterol binary mixtures: a 2D-ELDOR study. J. Phys. Chem. B. 111, 11260–11270.
Collado, M.I., Goni, F.M., Alonso, A., Marsh, D., 2005. Domain formation in sphingomyelin/cholesterol mixed membranes studied by spin-label electron spin resonance spectroscopy. Biochemistry 44, 4911–4918.
Conchello, J.A., Lichtman, J.W., 2005. Optical sectioning microscopy. Nat. Methods 2, 920–931.
Coste, V., Breton, M., Angelova, M.I., Puff, N., 2006. How to extract selectively the lo-phase domains from large unilamellar vesicles with Triton X-100? Colloids Surf. A 282–283, 402–409.
Coutinho, A., Prieto, M., 1993. Ribonuclease T1 and alcohol dehydrogenase fluorescence quenching by acrylamide: a laboratory experiment for undergraduate students. J. Chem. Educ. 70, 425–428.
Cremesti, A.E., Gõni, F.M., Kolesnick, R.N., 2002. Role of sphingomyelinase and ceramide in modulating rafts: do biophysical properties determine biological outcome? FEBS Lett. 531, 47–53.
Davenport, L., 1997. Fluorescence probes for studying membrane heterogeneity. Methods Enzymol. 278, 487–512.
Davey, A.M., Walvick, R.P., Liu, Y., Heikal, A.A., Sheets, E.D., 2007. Membrane order and molecular dynamics associated with IgE receptor cross-linking in mast cells. Biophys. J. 92, 343–355.
de Almeida, R.F.M., Fedorov, A., Prieto, M., 2003. Sphingomyelin/phosphatidylcholine/cholesterol phase diagram: boundaries and composition of lipid rafts. Biophys. J. 85, 2406–2416.
de Almeida, R.F.M., Borst, J., Fedorov, M., Prieto, A.J.W.G., Visser, 2007. Complexity of lipid domains and rafts in giant unilamellar vesicles revealed by combining imaging and microscopic and macroscopic time-resolved fluorescence. Biophys. J. 93, 539–553.
de Almeida, R.F.M., Loura, L.M.S., Fedorov, A., Prieto, M., 2002. Nonequilibrium phenomena in the phase separation of a two-component lipid bilayer. Biophys. J. 82, 823–834.
de Almeida, R.F.M., Loura, L.M.S., Fedorov, A., Prieto, M., 2005. Lipid rafts have different sizes depending on membrane composition: a time-resolved fluorescence resonance energy transfer study. J. Mol. Biol. 346, 1109–1120.
de Almeida, R.F.M., Loura, L.M.S., Prieto, M., Watts, A., Fedorov, A., Barrantes, F.J., 2004. Cholesterol modulates the organization of the γM4 transmembrane domain of the muscle nicotinic acetylcholine receptor. Biophys. J. 86, 2261–2272.
de Lange, M.J.L., Bonn, M., Müller, M., 2007. Direct measurement of phase coexistence in DPPC/cholesterol vesicles using Raman spectroscopy. Chem. Phys. Lipids 146, 76–84.
Degroote, S., Wolthoorn, J., Van Meer, G., 2004. The cell biology of glycosphingolipids. Semin. Cell Dev. Biol. 15, 375–387.
Devaux, P.F., Morris, R., 2004. Transmembrane asymmetry and lateral domains in biological membranes. Traffic 5, 241–246.
Dietrich, C., Bagatolli, L.A., Volovyk, Z.N., Thompson, N.L., Levi, M., Jacobson, K., Gratton, E., 2001. Lipid rafts reconstituted in model membranes. Biophys. J. 80, 1417–1428.
Digman, M.A., Caiolfa, V.R., Zamai, M., Gratton, E., 2008. The phasor approach to fluorescence lifetime imaging analysis. Biophys. J. 94, L14–16L. doi:10.1529/biophysj.107.120154.
Dong, C.Y., French, T., So, P.T.C., Buehler, C., Berland, K.M., Gratton, E., 1998. Fluorescence-lifetime imaging techniques for microscopy. Meth. Cell Biol. 72, 431–464.
Edidin, M., 2003. Lipids on the frontier: a century of cell-membrane bilayers. Nat. Rev. Mol. Cell Biol. 4, 414–418.
Elliott, R., Katsov, K., Schick, M., Szleifer, I., 2005. Phase separation of saturated and mono-unsaturated lipids as determined from a microscopic model. J. Chem. Phys. 122, 44904–44911.
Epand, R.M., 2006. The role of proteins in the formation of domains in membranes. In: Mateo, C.R., Gómez, J., Villalaín, J., González Ros, J.M. (Eds.), Protein–Lipid Interactions: New Approaches and Emerging Concepts. Springer, Berlin/Heidelberg, pp. 111–126.
Fernandes, F., Loura, L.M.S., Koehorst, R., Spruijt, R.B., Hemminga, M.A., Fedorov, A., Prieto, M., 2004. Quantification of protein–lipid selectivity using FRET: application to the M13 major coat protein. Biophys. J. 87, 344–352.
Fernandes, F., Loura, L.M.S., Prieto, M., Koehorst, R., Spruijt, R.B., Hemminga, M.A., 2003. Dependence of M13 major coat protein oligomerization and lateral segregation on bilayer composition. Biophys. J. 85, 2341–2430.
Filippov, A., Orädd, G., Lindblom, G., 2007. Domain formation in model membranes studied by pulsed-field gradient-NMR: the role of lipid polyunsaturation. Biophys. J. 93, 3182–3190.
Gasset, M., Killian, J.A., Tournois, H., de Kruijff, B., 1988. Influence of cholesterol on gramicidin-induced H_{II} phase formation in phosphatidylcholine model membranes. Biochim. Biophys. Acta 939, 79–88.
Goñi, F.M., Alonso, A., 2006. Biophysics of sphingolipids I. Membrane properties of sphingosine, ceramides and other simple sphingolipids. Biochim. Biophys. Acta 1758, 1902–1921.
Gratton, E., Breusegem, S., Sutin, J., Ruan, Q., Barry, N., 2003. Fluorescence lifetime imaging for the two-photon microscope: time-domain and frequency-domain methods. J. Biomed. Opt. 8, 381–390.
Halling, K.K., Ramstedt, B., Slotte, J.P., 2008. Glycosylation induces shifts in the lateral distribution of cholesterol from ordered towards less ordered domains. Biochim. Biophys. Acta 1778, 1100–1111.
Herreros, J., Ng, T., Schiavo, G., 2001. Lipid rafts act as specialized domains for tetanus toxin binding and internalization into neurons. Mol. Biol. Cell 12, 2947–2960.
Holt, A., de Almeida, R.F.M., Nyholm, T.K., Loura, L.M.S., Daily, A.E., Staffhorst, R.W., Rijkers, D.T., Koeppe 2nd., R.E., Prieto, M., Killian, J.A., 2008. Is there a preferential interaction between cholesterol and tryptophan residues in membrane proteins? Biochemistry 47, 2638–2649.
Hsueh, Y.-W., Chen, M.-T., Patty, P.J., Code, C., Cheng, J., Frisken, B.J., Zuckermann, M., Thewalt, J., 2007. Ergosterol in POPC membranes: physical properties and comparison with structurally similar sterols. Biophys. J. 92, 1606–1615.
Hsueh, Y.W., Gilbert, K., Trandum, C., Zuckermann, M., Thewalt, J., 2005. The effect of ergosterol on dipalmitoylphosphatidylcholine bilayers: a deuterium NMR and calorimetric study. Biophys. J. 88, 1799–1808.
Hudson, B.S., Cavalier, S.A., 1988. Studies of membrane dynamics and lipid–protein interactions with parinaric acid. In: Loew, L. (Ed.), Spectroscopic Membrane Probes, vol. I. CRC, Boca Raton, FL, pp. 43–62.
Ipsen, J.H., Karlstrom, G., Mouritsen, O.G., Wennerstrom, H., Zuckermann, M.J., 1987. Phase-equilibria in the phosphatidylcholine-cholesterol system. Biochim. Biophys. Acta 905, 162–172.
Ipsen, J.H., Mouritsen, O.G., Bloom, M., 1990. Relationships between lipid membrane area, hydrophobic thickness, and acyl-chain orientational order. The effects of cholesterol. Biophys. J. 57, 405–412.
Kahya, N., Schwille, P., 2006. Fluorescence correlation studies of lipid domains in model membranes. Mol. Membr. Biol. 23, 29–39.
Kolesnick, R.N., Gõni, F.M., Alonso, A., 2000. Compartmentalization of ceramide signaling: physical foundation and biological effects. J. Cell Physiol. 184, 285–300.
Korlach, J., Schwille, P., Webb, W.W., Feigenson, G.W., 1999. Characterization of lipid bilayer phases by confocal microscopy and fluorescence correlation spectroscopy. Proc. Natl. Acad. Sci. U.S.A. 96, 8461–8466.
Koynova, R., Caffrey, M., 1998. Phases and phase transitions of the phosphatidylcholines. Biochim. Biophys. Acta 1376, 91–145.
Kuerschner, L., Ejsing, C.S., Ekroos, K., Shevchenko, A., Anderson, K.I., Thiele, C., 2005. Polyene-lipids: a new tool to image lipids. Nat. Methods 2, 39–45.
Kusumi, A., Nakada, C., Ritchie, K., Murase, K., Suzuki, K., Murakoshi, H., Kasai, R.S., Kondo, J., Fujiwara, T., 2005. Paradigm shift of the plasma membrane concept from the two-dimensional continuum fluid to the partitioned fluid: high-speed single-molecule tracking of membrane molecules. Annu. Rev. Biophys. Biomolec. Struct. 34, 351–354.
Lakowicz, J.R., 2006. Principles of Fluorescence Spectroscopy, 3rd ed. Springer-Verlag, New York, NY.
Lentz, B.R., Barenholz, Y., Thompson, T.E., 1976. Fluorescence depolarization studies of phase transitions and fluidity in phospholipid bilayers 2. Two component phosphatidylcholine liposomes. Biochemistry 15, 4529–4537.
Lentz, B.R., Barrow, D.A., Hoechli, M., 1980. Cholesterol-phosphatidylcholine interactions in multilamellar vesicles. Biochemistry 19, 1943–1954.
Lentz, B.R., Burgess, S.W., 1989. A dimerization model for the concentration dependent photophysical properties of diphenylhexatriene and its phospholipid derivatives DPHpPC and DPHpPA. Biophys. J. 56, 723–733.
Lentz, B.R., 1988. Membrane "fluidity" from fluorescence anisotropy measurements. In: Loew, L. (Ed.), Spectroscopic Membrane Probes, vol. I. CRC, Boca Raton, FL, pp. 13–41.
Li, M., Reddy, L.G., Bennett, R., Silva Jr., N.D., Jones, L.R., Thomas, D.D., 1999. A fluorescence energy transfer method for analyzing protein oligomeric structure: application to phospholamban. Biophys. J. 76, 2587–2599.
Loura, L.M.S., Coutinho, A., Silva, A., Fedorov, A., Prieto, M., 2006. Structural effects of a basic peptide on the organization of dipalmitoylphosphatidylcholine/dipalmitoylphosphatidylserine membranes: a fluorescent resonance energy transfer study. J. Phys. Chem. B 2006 (110), 8130–8141.
Loura, L.M.S., de Almeida, R.F.M., Prieto, M., 2001a. Detection and characterization of membrane microheterogeneity by resonance energy transfer. J. Fluoresc. 11, 197–209.
Loura, L.M.S., Fedorov, A., Prieto, M., 2001b. Exclusion of a cholesterol analog from the cholesterol-rich phase in model membranes. Biochim. Biophys. Acta 1511, 236–243.
Loura, L.M.S., Fedorov, A., Prieto, M., 2001c. Fluid–fluid membrane microheterogeneity: a fluorescence resonance energy transfer study. Biophys. J. 80, 776–788.

Loura, L.M.S., Fedorov, A., Prieto, M., 2000. Partition of membrane probes in a gel/fluid two-component lipid system: a fluorescence resonance energy transfer study. Biochim. Biophys. Acta 1467, 101–112.
Margineanu, A., Hotta, J., Vallée, R.A.L., Van der Auweraer, M., Ameloot, M., Stefan, A., Beljonne, D., Engelborghs, Y., Herrmann, A., Müllen, K., De Schryver, F.C., Hofkens, J., 2007. Visualization of membrane rafts using a perylene monoimide derivative and fluorescence lifetime imaging. Biophys. J. 93, 2877–2891.
Marsh, D., 1990. Handbook of Lipid Bilayers. CRC, Boca Raton, FL.
Mateo, C.R., Acuna, A.U., Brochon, J.C., 1995. Liquid-crystalline phases of cholesterol lipid bilayers as revealed by the fluorescence of *trans*-parinaric acid. Biophys. J. 68, 978–987.
Mateo, C.R., Brochon, J.-C., Lillo, M.P., Acuña, A.U., 1993a. Lipid clustering in bilayers detected by the fluorescence kinetics and anisotropy of *trans*-parinaric acid. Biophys. J. 65, 2237–2247.
Mateo, C.R., Souto, A.A., Amat-Guerri, F., Acuna, A.U., 1996. New fluorescent octadecapentaenoic acids as probes of lipid membranes and protein–lipid interactions. Biophys. J. 71, 2177–2191.
Mathias, S., Peña, L.A., Kolesnick, R.N., 1998. Signal transduction of stress via ceramide. Biochem. J. 335, 465–480.
McMullen, T.P.W., McElhaney, R.N., 1995. New aspects of the interaction of cholesterol with dipalmitoylphosphatidylcholine bilayers as revealed by high-sensitivity differential scanning calorimetry. Biochim. Biophys. Acta 1234, 90–98.
Mukherjee, S., Chattopadhyay, A., 2005. Monitoring the organization and dynamics of bovine hippocampal membranes utilizing Laurdan generalized polarization. Biochim. Biophys. Acta 1714, 43–55.
Mukherjee, S., Maxfield, F.R., 2004. Membrane domains. Annu. Rev. Cell Dev. Biol. 20, 839–866.
Needham, D., Nunn, R.S., 1990. Elastic deformation and failure of lipid bilayer membranes containing cholesterol. Biophys. J. 58, 997–1009.
Nicolini, C., Baranski, J., Schlummer, S., Palomo, J., Lumbierres-Burgues, M., Kahms, M., Kuhlmann, J., Sanchez, S., Gratton, E., Waldmann, H., Winter, R., 2006a. Visualizing association of N-Ras in lipid microdomains: influence of domain structure and interfacial adsorption. J. Am. Chem. Soc. 128, 192–201.
Nicolini, C., Kraineva, J., Khurana, M., Periasamy, N., Funari, S.S., Winter, R., 2006b. Temperature and pressure effects on structural and conformational properties of POPC/SM/cholesterol model raft mixtures—a FT-IR, SAXS, DSC PPC and Laurdan fluorescence spectroscopy study. Biochim. Biophys. Acta 1758, 248–258.
Nicolau Jr., D.V., Burrage, K., Parton, R.G., Hancock, J.F., 2006. Identifying optimal lipid raft characteristics required to promote nanoscale protein–protein interactions on the plasma membrane. Mol. Cell. Biol. 26, 313–323.
O'Connor, D., Phillips, D., 1984. Time-correlated single photon counting. Academic, New York, NY.
Owen, D.M., Lanigan, P.M.P., Dunsby, C., Munro, I., Grant, D., Neil, M.A.A., French, P.M.W., Magee, A.I., 2006. Fluorescence lifetime imaging provides enhanced contrast when imaging the phase-sensitive dye di-4-ANEPPDHQ in model membranes and live cells. Biophys. J. 90, L80–L82.
Owen, D.M., Neil, M.A.A., French, P.M.W., Magee, A.I., 2007. Optical techniques for imaging membrane lipid microdomains in living cells. Semin. Cell Develop. Biol. 18, 591–598.
Parasassi, T., Ravagnan, G., Rusch, R.M., Gratton, E., 1993. Modulation and dynamics of phase properties in phospholipid mixtures detected by Laurdan fluorescence. Photochem. Photobiol. 57, 403–410.
Pérez-Gil, J., Cruz, A., de la Serna, J., 2006. Lateral membrane structure and lipid–protein interactions. In: Mateo, C.R., Gómez, J., Villalaín, J., González Ros, J.M. (Eds.), Protein–lipid Interactions: New Approaches and Emerging Concepts. Springer, Berlin/Heidelberg, pp. 127–140.
Prenner, E., Hermetter, A., Landl, G., Stutz, H., Kauffmann, H.F., Kungl, A.J., 1993. Fluorescence lifetime distributions of various phospholipids labeled with covalently bound diphenylhexatriene in the erythrocyte ghost membrane. J. Phys. Chem. 97, 2788–2792.
Prenner, E., Sommer, A., Maurer, N., Glatter, O., Gorges, R., Paltauf, F., Hermetter, A., 2000. Lateral microheterogeneity of diphenylhexatriene-labeled choline phospholipids in the erythrocyte ghost membrane as determined by time-resolved fluorescence spectroscopy. J. Membr. Biol. 174, 237–243.
Prior, I.A., Muncke, C., Parton, R.G., Hancock, J.F., 2003. Direct visualization of Ras proteins in spatially distinct cell surface microdomains. J. Cell Biol. 160, 165–170.
McQuaw, C.M., Zheng, L., Ewing, A.G., Winograd, N., 2007. Localization of sphingomyelin in cholesterol domains by imaging mass spectrometry. Langmuir 23, 5645–5650.
Rao, M., Mayor, S., 2005. Use of Forster's resonance energy transfer microscopy to study lipid rafts. Biochim. Biophys. Acta 1746, 221–233.
Razi-Naqvi, K., 1974. Diffusion-controlled reactions in two-dimensional fluids: discussion of measurements of lateral diffusion of lipids in biological membranes. Chem. Phys. Lett. 28, 280–284.
Ravichandra, B., Joshi, P.G., 1999. Gangliosides asymmetrically alter the membrane order in cultured PC-12 cells. Biophys. Chem. 76, 117–132.
Ruan, Q., Cheng, M.A., Levi, M., Gratton, E., Mantulin, W.W., 2004. Spatial-temporal studies of membrane dynamics: scanning fluorescence correlation spectroscopy (SFCS). Biophys. J. 87, 1260–1267.
Ruvolo, P.P., 2003. Intracellular signal transduction pathways activated by ceramide and its metabolites. Pharmacol. Res. 47, 383–392.
Sabatini, K., Mattila, J.-P., Kinnunen, P.K.J., 2008. Interfacial behavior of cholesterol, ergosterol, and lanosterol In mixtures with DPPC and DMPC monolayers. Biophys. J. 95, 2340–2355.
Sankaram, M.B., Thompson, T.E., 1990. Interaction of cholesterol with various glycerophospholipids and sphingomyelin. Biochemistry 29, 10670–10675.
Sankaram, M.B., Thompson, T.E., 1991. Cholesterol-induced fluid-phase immiscibility in membranes. Proc. Natl. Acad. Sci. U.S.A. 88, 8686–8690.
Santiago, J., Guzmàn, G.R., Rojas, L.V., Marti, R., Asmar-Rovira, G.A., Santana, L.F., McNamee, M., Lasalde-Dominicci, J.A., 2001. Probing the effects of membrane cholesterol in the Torpedo californica acetylcholine receptor and the novel lipid-exposed mutation alpha C418W in Xenopus oocytes. J. Biol. Chem. 276, 46523–46532.
Scherfeld, D., Kahya, N., Schwille, P., 2003. Lipid dynamics and domain formation in model membranes composed of ternary mixtures of unsaturated and saturated phosphatidylcholines and cholesterol. Biophys. J. 85, 3758–3768.
Sengupta, P., Holowka, D., Baird, B., 2007. Fluorescence resonance energy transfer between lipid probes detects nanoscopic heterogeneity in the plasma membrane of live cells. Biophys. J. 92, 3564–3574.
Sharma, M., Joshi, P.G., Joshi, N.B., 1997. Alterations in plasma membrane of glioblastoma cells by photodynamic action of merocyanine 540. Biochim. Biophys. Acta 1323, 272–280.
Sillen, A., Engelborghs, Y., 1998. The correct use of "average" fluorescence parameters. Photochem. Photobiol. 67, 475–486.
Silva, L.C., de Almeida, R.F.M., Castro, B.M., Fedorov, A., Prieto, M., 2007. Ceramide-domain formation and collapse in lipid rafts: membrane reorganization by an apoptotic lipid. Biophys. J. 92, 502–516.
Silva, L., Coutinho, A., Fedorov, A., Prieto, M., 2006a. Competitive binding of cholesterol and ergosterol to the polyene antibiotic nystatin: a fluorescence study. Biophys. J. 90, 3625–3631.
Silva, L.C., de Almeida, R.F.M., Matos, A.P., Fedorov, A., Prieto, M., 2006b. Ceramide-platform formation and -induced biophysical changes in a fluid phospholipid membrane. Mol. Membr. Biol. 23, 137–149.
Silvius, J.R., 2005. Partitioning of membrane molecules between raft and non-raft domains: insights from model-membrane studies. Biochim. Biophys. Acta 1746, 193–202.
Simons, K., Van Meer, G., 1988. Lipid sorting in epithelial-cells. Biochemistry 27, 6197–6202.
Sinha, M., Mishra, S., Joshi, P.G., 2003. Liquid-ordered microdomains in lipid rafts and plasma membrane of U-87 MG cells: a time-resolved fluorescence study. Eur. Biophys. J. 32, 381–391.
Sot, J., Bagatolli, L.A., Goñi, F.M., Alonso, A., 2006. Detergent-resistant ceramide-enriched domains in sphingomyelin/ceramide bilayers. Biophys. J. 90, 903–914.
Thewalt, J.L., Bloom, M., 1992. Phosphatidylcholine-cholesterol phase-diagrams. Biophys. J. 63, 1176–1181.
Towles, K.B., Brown, A.C., Wrenn, S.P., Dan, N., 2007. Effect of membrane microheterogeneity and domain size on fluorescence resonance energy transfer. Biophys. J. 93, 655–667.
Troup, G.M., Wrenn, S.P., 2004. Temperature and cholesterol composition-dependent behavior of 1-myristoyl-2-[12-[(5-dimethylamino-1-naphthalenesulfonyl)-amino]dodecan oyl]-*sn*-glycero-3-phosphocholine in 1,2-dimyristoyl-*sn*-glycero-3-phosphocholine membranes. Chem. Phys. Lipids 131, 167–182.
Umberger, J.Q., Lamer, V.K., 1945. The kinetics of diffusion controlled molecular and ionic reactions in solution as determined by measurements of the quenching of fluorescence. J. Am. Chem. Soc. 67, 1099–1109.
Valeur, B., 2001. Molecular Fluorescence: Principles and Applications. Wiley-VCH, Weinheim, Germany.
Van Duyl, B.Y., Meeldijk, H., Verkleij, A.J., Rijkers, D.T.S., Chupin, V., de Kruijff, B., Killian, J.A., 2005. A synergistic effect between cholesterol and tryptophan-flanked transmembrane helices modulates membrane curvature. Biochemistry 44, 4526–4532.
Van Meer, G., Liskamp, R.M., 2005. Brilliant lipids. Nat. Methods 2, 14–15.
Varma, R., Mayor, S., 1998. GPI-anchored proteins are organized in submicron domains at the cell surface. Nature 394, 798–801.
Vaz, W.L.C., Melo, E., 2002. Fluorescence spectroscopic studies on phase heterogeneity in lipid bilayer membranes. J. Fluoresc. 11, 255–271.
Veatch, S.L., Gawrisch, K., Keller, S.L., 2006. Closed-loop miscibility gap and quantitative tie-lines in ternary membranes containing diphytanoyl PC. Biophys. J. 90, 4428–4436.
Veatch, S.L., Keller, S.L., 2003. Separation of liquid phases in giant vesicles of ternary mixtures of phospholipids and cholesterol. Biophys. J. 85, 3074–3083.
Veatch, S.L., Polozov, I.V., Gawrisch, K., Keller, S.L., 2004. Liquid domains in vesicles investigated by NMR and fluorescence microscopy. Biophys. J. 86, 2910–2922.
Veatch, S.L., Soubias, O., Keller, S.L., Gawrisch, K., 2007. Critical fluctuations in domain-forming lipid mixtures. Proc. Natl. Acad. Sci. U.S.A. 104, 17650–17655.
Velez, M., Lillo, M.P., Acuna, A.U., Gonzalezrodriguez, J., 1995. Cholesterol effect on the physical state of lipid multibilayers from the platelet plasma-membrane by time-resolved fluorescence. Biochim. Biophys. Acta 1235, 343–350.
Visser, A.J.W.G., Vos, K., Vanhoek, A., Santema, J.S., 1988. Time-resolved fluorescence depolarization of rhodamine-B and octadecylrhodamine-B in Triton X-100 micelles and aerosol Ot reversed micelles. J. Phys. Chem. 92, 759–765.
Vist, M.R., Davis, J.H., 1990. Phase equilibria of cholesterol/dipalmitoylphosphatidylcholine mixtures: ^{2}H nuclear magnetic resonance and differential scanning calorimetry. Biochemistry 29, 451–464.

Von Arnim, C.A.F., Kinoshita, A., Peltan, I.D., Tangredi, M.M., Herl, L., Lee, B.M., Spoelgen, R., Hshieh, T.T., Ranganathan, S., Battey, F.D., Liu, C.X., Bacskai, B.J., Sever, S., Irizarry, M.C., Strickland, D.K., Hyman, B.T., 2005. The low density lipoprotein receptor-related protein (LRP) is a novel beta-secretase (BACE1) substrate. J. Biol. Chem. 280, 17777–17785.

Wolber, P.K., Hudson, B.S., 1982. Bilayer acyl chain dynamics and lipid–protein interaction—the effect of the bacteriophage-M13 coat protein on the decay of the fluorescence anisotropy of parinaric acid. Biophys. J. 37, 253–262.

Wolf, D., 1988. Probing the lateral organization and dynamics of membranes. In: Loew, L. (Ed.), Spectroscopic Membrane Probes, vol. I. CRC, Boca Raton, FL, pp. 193–220.

Wu, R., Chen, L., Yu, Z., Quinn, P.J., 2006. Phase diagram of stigmasterol-dipalmitoylphosphatidylcholine mixtures dispersed in excess water. Biochim. Biophys. Acta 1758, 764–771.

Wustner, D., 2007. Fluorescent sterols as tools in membrane biophysics and cell biology. Chem. Phys. Lipids 146, 1–25.